THE SENSITIVITY OF EVAPORATION RATE TO CLIMATE CHANGE--

RESULTS OF AN ENERGY-BALANCE APPROACH

By Larry Benson

U.S. GEOLOGICAL SURVEY

Water-Resources Investigations Report 86-4148

Denver, Colorado
1986

UNITED STATES DEPARTMENT OF THE INTERIOR

DONALD PAUL HODEL, Secretary

GEOLOGICAL SURVEY

Dallas L. Peck, Director

For additional information
write to:

L. Benson, Project Chief
U.S. Geological Survey
Box 25046, Mail Stop 403
Denver Federal Center
Denver, CO 80225
Telephone: (303) 236-5917

For sale by:

Open-File Services Section
Western Distribution Branch
U.S. Geological Survey
Box 25425, Mail Stop 306
Denver Federal Center
Denver, CO 80225
Telephone: (303) 236-7476

CONTENTS

FIGURES

TABLES

SYMBOLS, VARIABLES, DIMENSIONS, AND DEFINITIONS
USED IN EQUATIONS AND EVAP COMPUTER PROGRAM

A_j	-	- (cm^2)	area of the jth layer of water.
A_{hl}	- ALBHI	- (dimensionless)	albedo of high-altitude cirrus clouds; $A_{hl} = 0.21$.
A_l	-	- (cm^2)	area of lake.
A_{ll}	- ALBLO	- (dimensionless)	albedo of low-level heap clouds; $A_{ll} = 0.70$.
A_{ml}	- ALBMED	- (dimensionless)	albedo of medium-altitude clouds; $A_{ml} = 0.48$.
a_{hl}	- AH	- (dimensionless)	$a_{hl} = 0.74+f_{hl}(0.025\chi e^{-0.1916\alpha_{hl}})$.
a_{ll}	- AL	- (dimensionless)	$a_{ll} = 0.74+f_{ll}(0.025\chi e^{-0.1916\alpha_{ll}})$.
a_{ml}	- AM	- (dimensionless)	$a_{ml} = 0.74+f_{ml}(0.025\chi e^{-0.1916\alpha_{ml}})$.
α_{hl}	- ALTHI	- (dimensionless)	altitude of high-level clouds; $\alpha_{hl} = 6$ km.
α_{ll}	- ALTLO	- (dimensionless)	altitude of low-level clouds; $\alpha_{ll} = 1$ km.
α_{ml}	- ALTMED	- (dimensionless)	altitude of medium-level clouds; $\alpha_{ml} = 4$ km.
b_{hl}	- BH	- (dimensionless)	$b_{hl} = 0.00490-f_{hl}\ (0.00054\chi e^{-0.1969\alpha_{hl}})$.
b_{ll}	- BL	- (dimensionless)	$b_{ll} = 0.00490-f_{ll}\ (0.00054\chi e^{-0.1969\alpha_{ll}})$.
b_{ml}	- BM	- (dimensionless)	$b_{ml} = 0.00490-f_{ml}\ (0.00054\chi e^{-0.1969\alpha_{ml}})$.
β	- BOWRAT	- (dimensionless)	Bowen ratio; the ratio of the energy conducted to (or from) the air as sensible heat to energy used for evaporation (latent heat).
C_e	-	- (dimensionless)	bulk-vaporation coefficient.
C_m	-	- (dimensionless)	mass-transfer coefficient.
C_w	-	- (cal g^{-1} $°K^{-1}$)	specific heat of water; $C_w \tilde{-} 1.0$.
c_p	-	- (cal g^{-1} $°K^{-1}$	specific heat of air at constant pressure.
$\bar{d}\ d^{-1}$	-	- (dimensionless)	ratio of the mean Earth-sun distance to the instantaneous distance; $\bar{d}\ d^{-1} \tilde{-} 1.0$.

d_0	- D0	- (dimensionless)	d_0 = 6984.505294.
d_1	- D1	- (dimensionless)	d_1 = -188.9039310.
d_2	- D2	- (dimensionless)	d_2 = 2.133357675.
d_3	- D3	- (dimensionless)	d_3 = -1.288580973E-2.
d_4	- D4	- (dimensionless)	d_4 = 4.393587233E-5.
d_5	- D5	- (dimensionless)	d_5 = -8.023923082E-8.
d_6	- D6	- (dimensionless)	d_6 = 6.136820929E-11.
D_g	-	- (cm^3)	ground-water discharge into lake.
D_r	-	- (cm^3)	runoff into lake.
Δ	-	- (dimensionless)	slope of saturation water-vapor curve.
E	-	- ($cm\ yr^{-1}$)	evaporation rate.
E_v	-	- ($cm^3\ cm^{-2}\ s^{-1}$)	eddy-vapor flux.
E_1	- EVAP	- ($cm\ d^{-1}$)	daily evaporation rate.
E_{30}	- MEVAP	- ($cm\ mo^{-1}$)	monthly evaporation rate.
E_{365}	- ANEVAP	- ($m\ yr^{-1}$)	annual evaporation rate.
e	-	- (dimensionless)	Napierian logarithm base; e = 2.7183.
$\tilde{e}$	-	- (dimensionless)	the emissivity of water at water-surface temperature, T_o; $\tilde{e} \sim 0.97$.
e_a	- MVP	- (mb)	vapor pressure of the air, for the actual condition of humidity.
e_o	- SVPOM	- (mb)	vapor pressure of saturated air at temperature, T_o, of the water surface.
e_s	- SVP2M	- (mb)	vapor pressure of saturated air at the observed air temperature, T_a.
f_{hl}	- FRHI	- (dimensionless)	fraction of sky covered by high-altitude clouds.
f_{ll}	- FRLO	- (dimensionless)	fraction of sky covered by low-altitude clouds.
f_{ml}	- FRMED	- (dimensionless)	fraction of sky covered by medium-altitude clouds.
γ	-	- (dimensionless)	psychrometric constant.

γ^*	-	- (degrees)	solar altitude, the angle of the sun above the horizon.
L	- LHEAT	- (cal g^{-1})	latent heat of vaporization of water at temperature, T_o.
λ	-	- (cal cm^{-2})	Langley; the energy unit of solar radiation; λ = 1 cal cm^{-2}.
$\bar{M}$	- MASSAIR	- (dimensionless)	mean optical air mass, the length of the atmospheric path traversed by the sun's rays in reaching the Earth, measured in terms of the length of this path when the sun is in the zenith.
P	- P	- (mb)	atmospheric pressure at a standard distance above the water surface.
P_l	-	- (cm)	precipitation that falls on lake.
Q*	- QSTAR	- (cal cm^{-2} d^{-1})	solar irradiation incident on the upper atmosphere at a specified latitude.
Q_a	- QA	- (cal cm^{-2} d^{-1})	long-wave radiation falling on the water surface from the atmosphere.
$Q_{a,hl}$	- QAH	- (cal cm^{-2} d^{-1})	long-wave radiation falling on the water surface from high-level clouds.
$Q_{a,ll}$	- QAL	- (cal cm^{-2} d^{-1})	long-wave radiation falling on the water surface from low-level clouds.
$Q_{a,ml}$	- QAM	- (cal cm^{-2} d^{-1})	long-wave radiation falling on the water surface from medium-level clouds.
Q_{ar}	- QAR	- (cal cm^{-2} d^{-1})	the part of the incoming long-wave radiation that is reflected from the water surface back to the atmosphere.
Q_{bs}	- QBS	- (cal cm^{-2} d^{-1})	long-wave radiation emitted by the body of water; the numerical value of Q_{bs} is determined by the surface temperature of the water.
Q_e	-	- (cal cm^{-2} d^{-1})	energy flux resulting from a change in the latent heat content of evaporating water.
Q_h	-	- (cal cm^{-2} d^{-1})	energy flux conducted from the water as sensible heat (enthalpy) during evaporation.
Q_r	- QR	- (cal cm^{-2} d^{-1})	the part of the incoming solar radiation that is reflected from the water surface.

Q_s	- QS	- (cal cm^{-2} d^{-1})	solar radiation incident to the water surface.
Q_v	- QV	- (cal cm^{-2} d^{-1})	net heat energy brought (advected) into the body of water by all surface- and ground-water sources and sinks.
Q_ν	-	- (cal)	net heat stored in body of water.
Q_w	-	- (cal cm^{-2} d^{-1})	energy flux resulting from advection of evaporating water.
q	-	- (dimensionless)	specific humidity.
q'	-	- (dimensionless)	difference between turbulent fluctuation in specific humidity and its mean value.
q_o	-	- (dimensionless)	saturation-specific humidity at water-surface temperature.
ΔQ_ν	- QNU	- (cal cm^{-2} d^{-1})	change in the energy stored in the body of water.
R_a	-	- (dimensionless)	long-wave reflectivity of the water surface; $R_a \tilde{-} 0.030$.
R_n	-	- (cal cm^{-2} s^{-1})	net radiative flux density reaching water surface.
R_s	-	- (dimensionless)	solar-radiation reflectivity of the water surface; $R_S \tilde{-} 0.07$.
RH	- HUMID	- (dimensionless)	relative humidity; ratio of the actual water vapor present in a parcel of air to that which would be present at saturation.
ρ_a	-	- (g cm^{-3})	air density.
ρ_e	-	- (g cm^{-3})	density of water undergoing evaporation.
ρ_j	-	- (g cm^{-3})	density of jth layer of lake water.
ρ_v	-	- (g cm^{-3})	density of advected surface and ground water.
S	-	- (cal cm^{-2} min^{-1})	the solar constant; S = 1.94.
σ	-	- (cal cm^{-2} d^{-1} $^oK^{-1}$)	Stefan's constant; $\sigma = 11.71 \times 10^{-8}$.
$\bar{t}$	-	- (h)	duration of sunshine at a specific latitude.

T_a	- AIRT	- (°K)	temperature of the air at a standard distance above the body of water.
T_b	- BASET	- (°K)	arbitrary base temperature of the body of water; T_b = 273.15°K.
$\overline{T}_i$	-	- (°K)	mean temperature of ith source of advected water.
$\overline{T}_j$	-	- (°K)	mean temperature of jth layer of lake water.
T_o	- WATERT	- (°K)	surface temperature of the body of water undergoing evaporation.
T_{dp}	- DEWPT	- (°K)	dewpoint temperature, the temperature to which a parcel of air must be cooled at constant pressure and water-vapor content to achieve saturation.
Υ_{ab}	- TAUALB	- (dimensionless)	atmospheric transmission coefficient resulting from cloud albedo.
Υ_{da}	- TAUDRY	- (dimensionless)	atmospheric transmission coefficient resulting from dry-air scattering.
Υ_{wa}	- TAUWET	- (dimensionless)	atmospheric transmission coefficient resulting from water-vapor absorption.
Υ_{ws}	- TAUSCAT	- (dimensionless)	atmospheric transmission coefficient resulting from water-vapor scattering.
u	-	- (cm s^{-1})	wind velocity.
V_i	-	- (cm^3)	volume of water input to the lake from the ith surface- or ground-water source.
W	- WLOFT	- (cm)	precipitable water aloft, (that is, total water-vapor content of the air at all levels).
w'	-	- (cm s^{-1})	difference between turbulent fluctuation in vertical windspeed and mean value.
Ω	-	- (dimensionless)	constant in the Priestly-Taylor equation.
Δx_j	-	- (cm)	thickness of the jth layer of water.
χ	- SKY	- (dimensionless)	fraction of sky covered with clouds.
$\overline{Z}$	-	- (degrees)	zenith angle, the angular distance of the sun from the local vertical.

CONVERSION TABLE

The SI units (International System of units) used in this report may be converted to inch-pound units by use of the following conversion factors:

Multiply SI units	*By*	*To obtain inch-pound units*
micrometer (μm)	3.937×10^{-5}	inch
centimeter (cm)	0.3937	inch
meter (m)	3.281	foot
kilometer (km)	6.214×10^{-1}	mile
centimeter squared (cm^2)	0.1550	inch squared
kilometer squared (km^2)	0.3861	mile squared
centimeter cubed (cm^3)	0.06102	inch cubed
kilometer cubed (km^3)	0.2399	mile cubed
gram (g)	0.2205×10^{-2}	pound
meter per year ($m\ yr^{-1}$)	3.281	feet per year
cubic kilometer per year ($km^3\ yr^{-1}$)	0.2397	cubic miles per year

To convert degrees Celsius (°C) to degrees Fahrenheit (°F) use the following formula: °F=9/5 °C+32.

THE SENSITIVITY OF EVAPORATION RATE TO CLIMATE CHANGE-- RESULTS OF AN ENERGY-BALANCE APPROACH

By Larry Benson

ABSTRACT

This paper documents research indicating a reduction in mean-annual evaporation rate was probably necessary for the creation of Great Basin paleolake systems, which were at their highest levels 17,000 to 12,500 years before present. A review of various methods used to estimate evaporation rate indicates that the energy-balance method is preferred for paleoclimatic application. An energy-balance model (EVAP) was used to calculate the sensitivity of evaporation rate to changes in commonly measured climate parameters. Results of the analysis indicate evaporation rate is strongly dependent on the difference between air and water-surface temperatures, the type of clouds, and the degree of cloudiness. Neither changes in solar irradiation nor changes in relative humidity exert significant changes in the calculated evaporation rate.

INTRODUCTION

During the past 20,000 years, radical changes occurred in the size of lakes located in the western Great Basin of the United States. These changes, resulting from variations in the hydrologic balance, were in part due to changes in evaporation rate. The purpose of this study is to estimate the sensitivity of evaporation rate to variation in values of parameters commonly used to describe climate. In realizing this purpose, we can begin to set quantitative bounds on the magnitudes and rates of climate change that have occurred in the western Great Basin in the past and that may occur in the future.

Changes in the Surface Altitudes of Great Basin Lakes

Well-documented lake-level chronologies exist for three Great Basin paleolake systems: Lake Russell in California, Lake Lahontan in Nevada and California, and Lake Bonneville in Utah (fig. 1). The timing of the last high lake level (highstand) of Lake Russell in the Mono drainage basin and of Lake Lahontan in the Lahontan drainage basin is nearly identical, occurring about 14,000 to 12,500 years before present (yr B.P.); Lake Bonneville appears to have achieved a highstand at a slightly earlier period, about 17,000 to 14,000 yr B.P. (fig. 2).

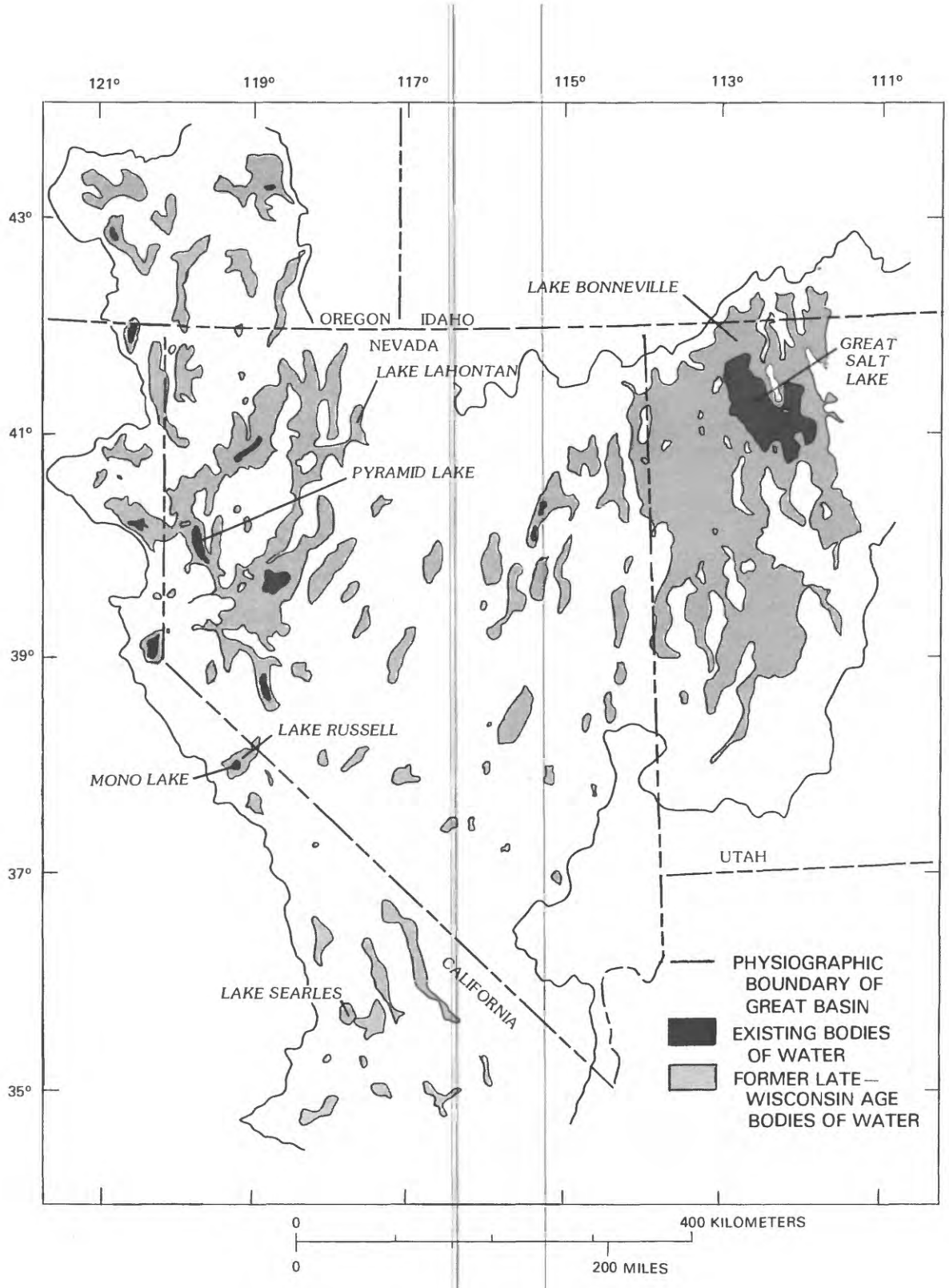

Figure 1.--Late Pleistocene lakes of the Great Basin (modified after Spaulding and others, 1983).

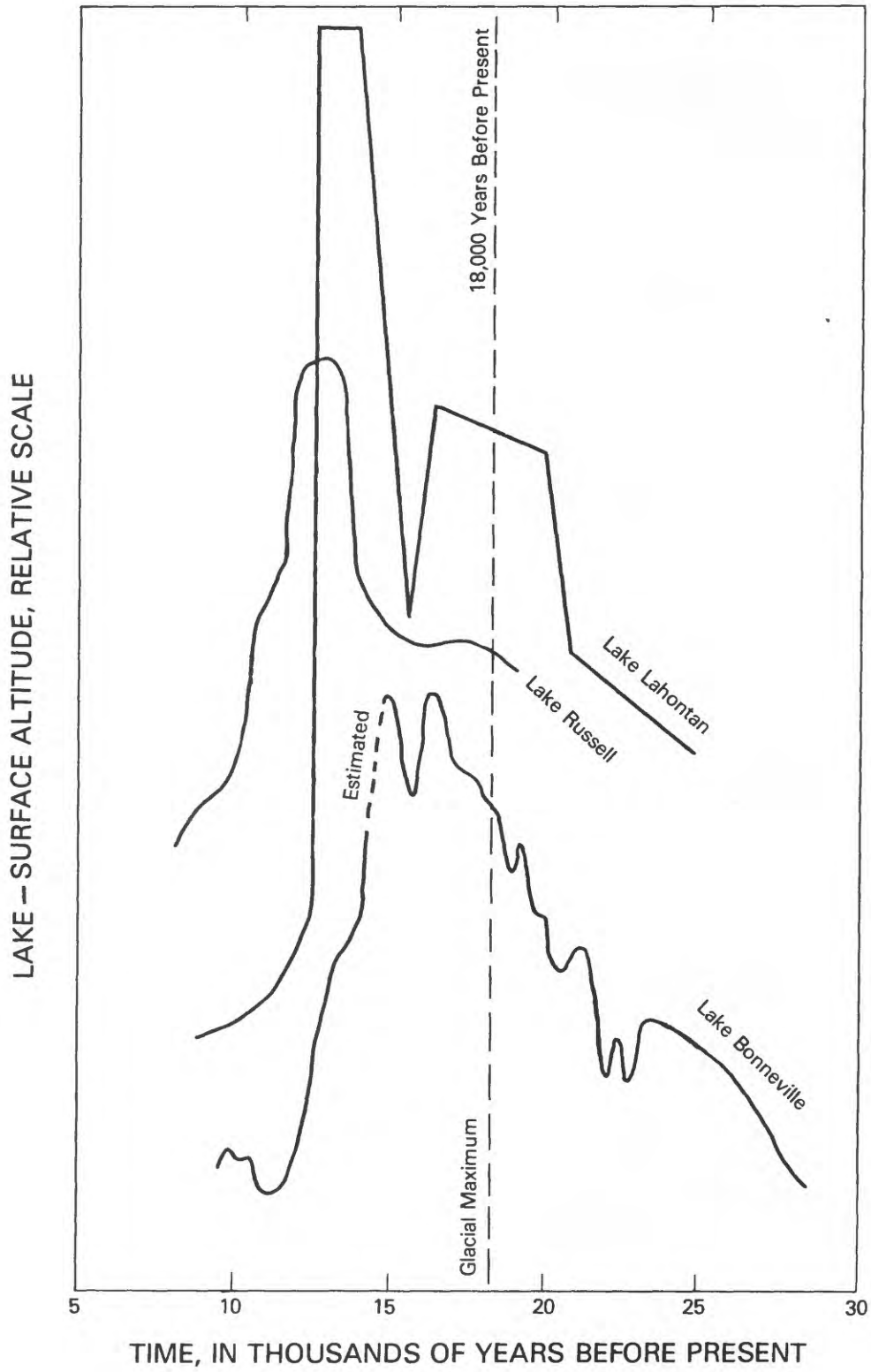

Figure 2.--Fluctuations in lake-surface altitudes for Lake Russell (K. W. Lajoie, U.S. Geological Survey, written commun., 1985), Lake Lahontan (Thompson and others, 1986), and Lake Bonneville (Curry and Oviatt, 1985).

The difference in timing may be the result of differences in the geographical settings of the Mono, Lahontan, and Bonneville drainage basins, combined with the variability in time and space of climate change; or the difference may be the result of incorrect assumptions used in the calculation of radiocarbon ages of carbonate and woody materials associated with the highstands. However, for the purposes of this study, the timing is not as important as the magnitude of change in lake size that occurred during the transition from a highstand to a lowstand.

What was the climate during the last highstand? Was it colder, wetter, or cloudier than the climate of today (1985)? Very little is known about climate during the late Wisconsin. Dohrenwend's (1984) study of nivation landforms in the western Great Basin indicates mean annual temperatures were about 7 °K lower during the full glacial compared to today. This assumption is supported by studies conducted in the eastern part of the Great Basin by Thompson and Meade (1982) and Thompson (1984). These studies determined that the lower limit of subalpine and woodland conifers lowered about 1,000 m during the full glacial; this lowering implies a minimum reduction in summer temperatures of 5 to 6 °K. These estimates of full-glacial air temperature, however, are not sufficient for an understanding of changes in the hydrologic balance that led to the formation of the highstand lakes. Runoff data, precipitation data, and evaporation-rate data for highstand periods also are needed. Lacking such data, another approach is adopted, where it is assumed that available historical-data sets record certain events that are representative of the hydrologic and meteorologic conditions that existed during the time of a highstand lake. Thus, an analogy is made between the climate of a single year and the average climate that persisted for several hundred to a few thousand years in the distant past.

Change in the Size of Lakes in the Lahontan Basin, 12,500 to 12,000 years before present

We have chosen to work with the Lahontan basin, because of the availability of bathymetric data (Benson and Mifflin, 1985), precipitation data (U.S. Weather Bureau, 1950-65; National Oceanic and Atmospheric Administration, 1966-75), runoff data (U.S. Geological Survey, 1884-1950, 1950-60, 1961-83), and lake-level data (Benson, 1978, 1981; Thompson and others, 1986). About 12,500 yr B.P., Lake Lahontan existed as a single body of water with a surface altitude of 1,330 m. The lake at its deepest point was 278 m and had a surface area of 22,300 km^2 and a volume of 2,020 km^3. Radiocarbon ages of tufa, gastropod, and fossil plant samples (Born, 1972; Benson, 1981; and Thompson and others, 1986) from the adjoining Pyramid and Winnemucca Dry Lake subbasins (fig. 3) indicate that by 12,000 yr B.P., Lake Lahontan had fallen to a level (1,180 m) similar to that observed by King (1878) in 1867. The combined surface area of lakes existing in the seven Lahontan subbasins at that time was about 1,550 km^2. Assuming the combined surface areas of lakes to be similar in 1882 and 12,000 yr B.P., the decline in lake level between 12,500 and 12,000 yr B.P. was determined to be associated with a 93-percent reduction in surface area.

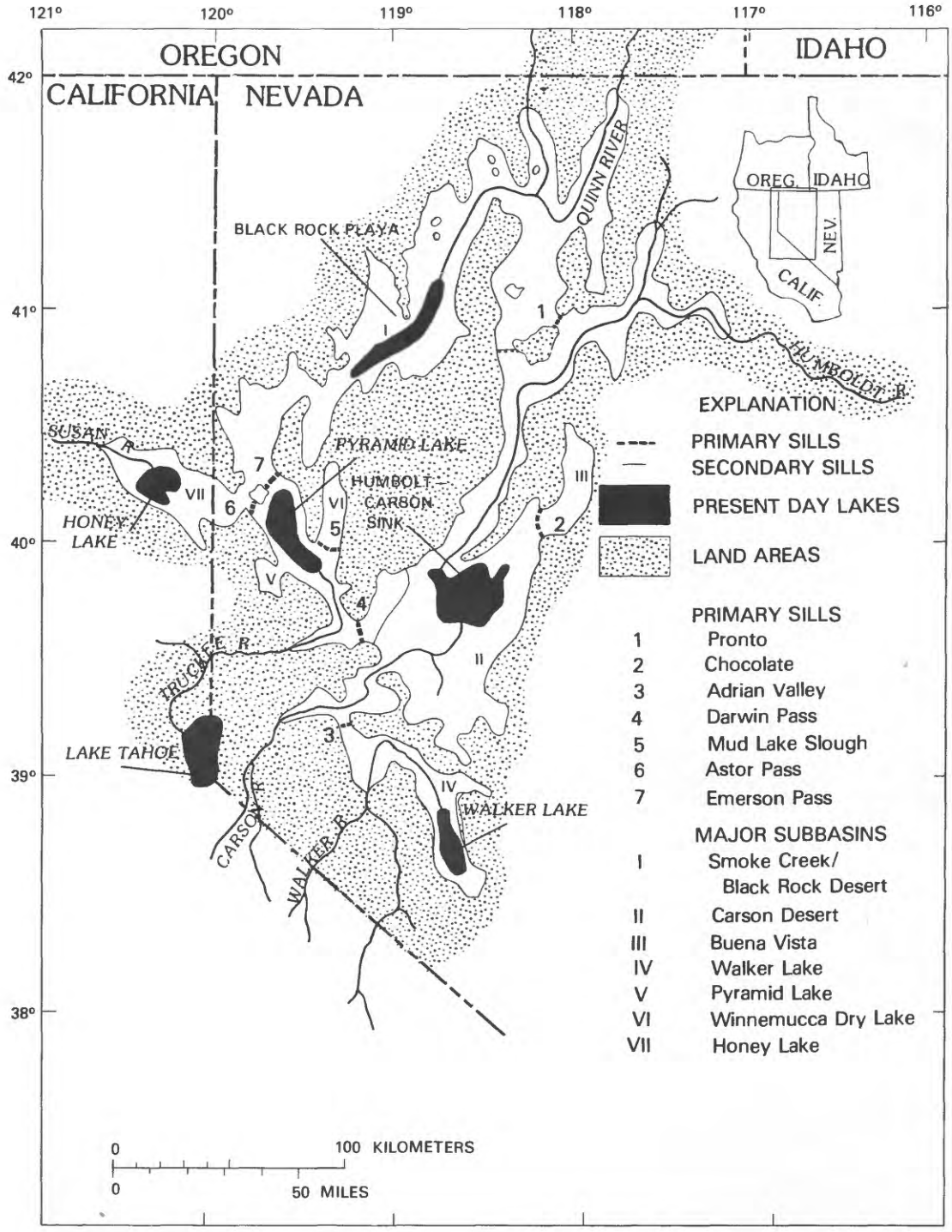

Figure 3.--Surface area of Lake Lahontan 14,000 to 12,500 years before present and location of subbasins and sills separating subbasins.

The steady-state hydrologic balance for a closed-basin lake can be written:

$$E_l A_l = P_l A_l + D_r + D_g \quad (1)$$

where E_l is lake-evaporation rate,

A_l is surface area of the lake,

P_l is precipitation on the lake,

D_r is surface-water runoff into the lake, and

D_g is net ground-water discharge into the lake.

For the Lahontan basin, $D_g << D_r$ (Everett and Rush, 1967; Van Denburgh and others, 1973). From equation (1): an increase in the surface area of Lake Lahontan primarily was the result of increased precipitation on the lake surface, increased surface-water runoff to the lake basin, decreased evaporation rate acting on the lake surface, or a combination of these factors. The role of increased precipitation and runoff in the creation and maintenance of the highstand of Lake Lahontan 12,500 yr B.P. can be assessed if values for mean annual discharge and precipitation 12,500 yr B.P. can be assumed to have been identical with a particularly "wet" year for which data are available. This assumption is somewhat arbitrary in that historical values of surface-water runoff and precipitation for an extremely wet year may be larger or smaller than mean values characteristic of runoff and precipitation 12,500 yr B.P. However, use of extreme values from the historical record of climate as proxies for Pleistocene climate, to a limited extent, is supported by Bryson and Hare (1974) and LaMarche (1974). Bryson and Hare state "***Late Pleistocene monthly climatic means appear to have been not much different than extreme individual months at the present time. It apparently takes only a changed frequency and combination of present-day weather patterns to produce an ice-age climate."

Streamflow for three of the four major rivers (the Carson, Humboldt, and Truckee Rivers) that discharge to the Lahontan basin (fig. 4) are available for 1942-82; however, discharge data for the fourth major river, the Walker River, only are available for 1958-77. Considering only the time span for which discharge data are available for all four rivers, these data indicate that extremely high runoff occurred during 1969 (fig. 5).

Streamflow data for all six rivers that discharge to the Lahontan basin--the Carson, Humboldt, Quinn, Susan, Truckee, and Walker Rivers--as well as precipitation data from nine basin-floor weather stations (see fig. 4 for location of streamflow-gaging and weather stations) were assembled for 1969 (tables 1 and 2). These data, with water-balance estimates of historical mean-annual evaporation rates (Harding, 1965), were used to estimate the hypothetical surface areas of lakes that would be created in Lahontan subbasins as the result of an increase in mean-annual fluid input equal to 1969 values, while leaving the value of the mean-annual evaporation rate unchanged from its historical value. The combined surface area of lakes in the Lahontan basin

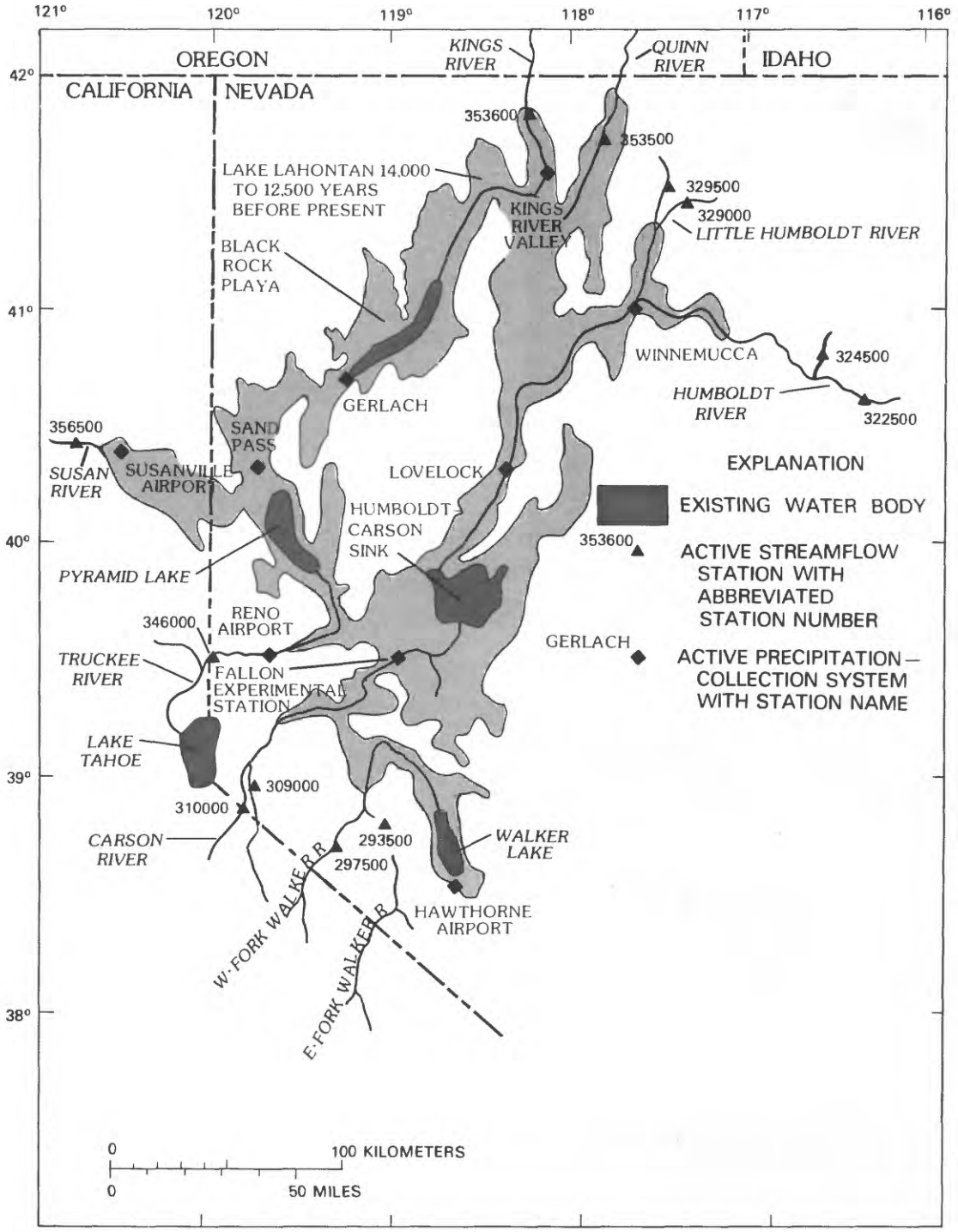

Figure 4.--Location of streamflow-gaging and weather stations for which data are available for 1969.

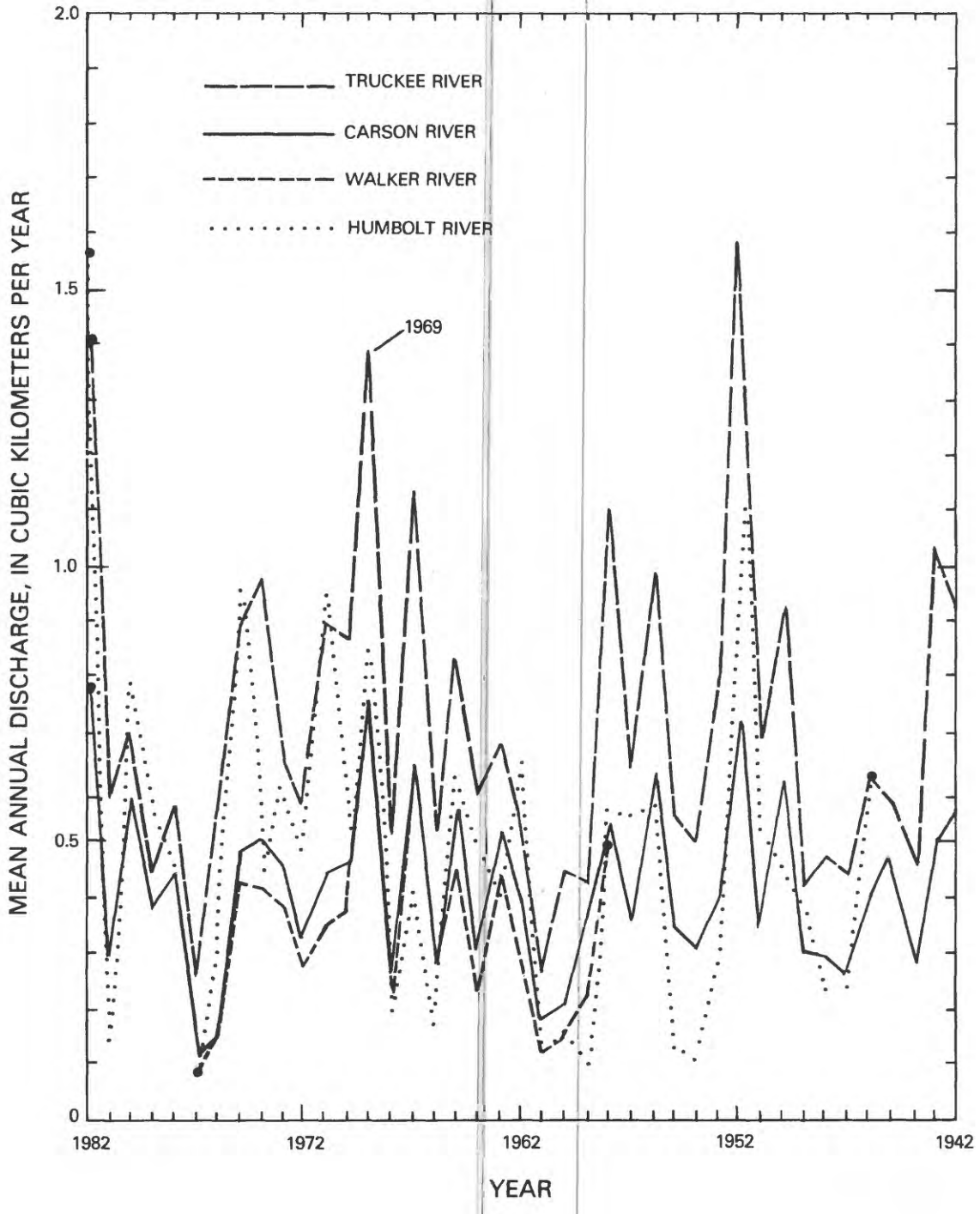

Figure 5.--Mean annual discharge for the Carson (1942-82), Truckee (1942-82), Humboldt (1946-82), and Walker Rivers (1958-77).

Table 1.--*Streamflow statistics for rivers that discharge to the Lahontan basin*

[$km^3\ yr^{-1}$, cubic kilometers per year]

River name	Streamflow-gaging station number	Sample size (complete data sets)	Mean streamflow discharge ($km^3\ yr^{-1}$)	1969 streamflow discharge ($km^3\ yr^{-1}$)
Carson River----	10309000	57	0.352	0.614
	10310000	52	.102	.156
Humboldt River--	10322500	76	.344	.546
	10324500	43	.033	.112
	10329000	45	.022	.064
	10329500	62	.030	.059
			[1].580	[1].580
Quinn River-----	10353500	34	.032	.077
	10353600	13	.004	[2].010
Susan River-----	10356500	34	.085	.153
Truckee River---	10346000	84	.725	1.390
Walker River----	10293500	31	.127	.365
	10297500	36	.213	.417
			[1].039	[1].039

[1]Estimated consumptive use occurring upstream from streamflow-gaging stations; evapotranspiration rate of 1 meter per year used in estimate.
[2]Estimate made by regression.

Table 2.--*Precipitation statistics for weather stations located on the floor of the Lahontan basin*

[yr, years; cm, centimeters; $\bar{x}$, mean; σ, standard deviation]

Weather-station name	Record length (yr)	Sample size (complete data sets)	Precipitation statistics (cm) $\bar{x}$	Precipitation statistics (cm) σ	1969 precipitation (cm)
Fallon Experimental Station	78	77	12.7	4.2	14.8
Gerlach----------	38	38	15.6	6.8	26.1
Hawthorne Airport----------	47	37	13.5	4.3	18.7
Kings River Valley---------	28	21	23.5	5.9	26.4
Lovelock----------	91	68	13.7	5.6	19.2
Reno Airport----------	123	123	17.9	6.6	26.0
Sand Pass----------	59	48	16.4	4.8	24.6
Susanville Airport---------	57	56	38.3	12.5	50.7
Winnemucca----------	114	114	21.3	6.1	25.6
Yerrington----------	71	62	13.2	4.8	20.9

resulting from this hypothetical situation total 3,680 km^2 (fig. 6), only one-sixth of the surface area that existed during the last highstand. To create the last highstand lake, using 1969 values of fluid input, the basin-wide evaporation rate needs to be reduced from its mean-annual value of 1.24 m/yr^{-1} to 0.46 m/yr^{-1}. These calculations demonstrate the potential importance of evaporation rate as a factor in creating the large paleolake systems that existed in the Great Basin 17,000 to 12,500 yr B.P.

The following section summarizes the evaluations that were made of the various methods for calculating evaporation rate preparatory to choosing one for subsequent sensitivity calculations. The choice of method was decided principally by the need for application to paleolake and paleoclimate conditions. The main objective was to estimate differences in evaporation rate (relative to historical mean values) in terms of observable and commonly measured climatic characteristics, such as cloudiness, air temperature, water temperature, and humidity.

METHODS FOR THE CALCULATION OF EVAPORATION RATE

For the purposes of this study, evaporation is defined as the transfer of water vapor from a free-water surface into the atmosphere. A number of methods are available for the computation or estimation of evaporation: Covariance, aerodynamic (mass-transfer), Dalton, energy-balance, combination, and empirical methods. A part of the discussion in these sections is modified from Brutsaert (1984).

Covariance Methods

In terms of accuracy, covariance (eddy correlation) methods provide the most accurate method of measuring evaporation. They also are the most direct methods for the determination of evaporation, in that they involve measurement of the actual vertical vapor flux. The principle behind the method is that downward-moving air will have a lower vapor pressure than upward-moving air over an evaporating surface because vapor movement occurs by a turbulent transport process. In essence, the turbulent diffusion equation (eq. 2) is written in the form of a molecular-transfer process in which turbulent instead of laminar boundary layers occur.

$$E_v = \overline{(\rho_a w')q'} \qquad (2)$$

where E_v is the eddy vapor flux,

ρ_a is the air density,

w' represents the difference between the instantaneous vertical wind speed and its mean value,

q' represents the difference between the instantaneous specific humidity and its mean value, and

$\overline{\quad}$ denotes mean value with respect to time.

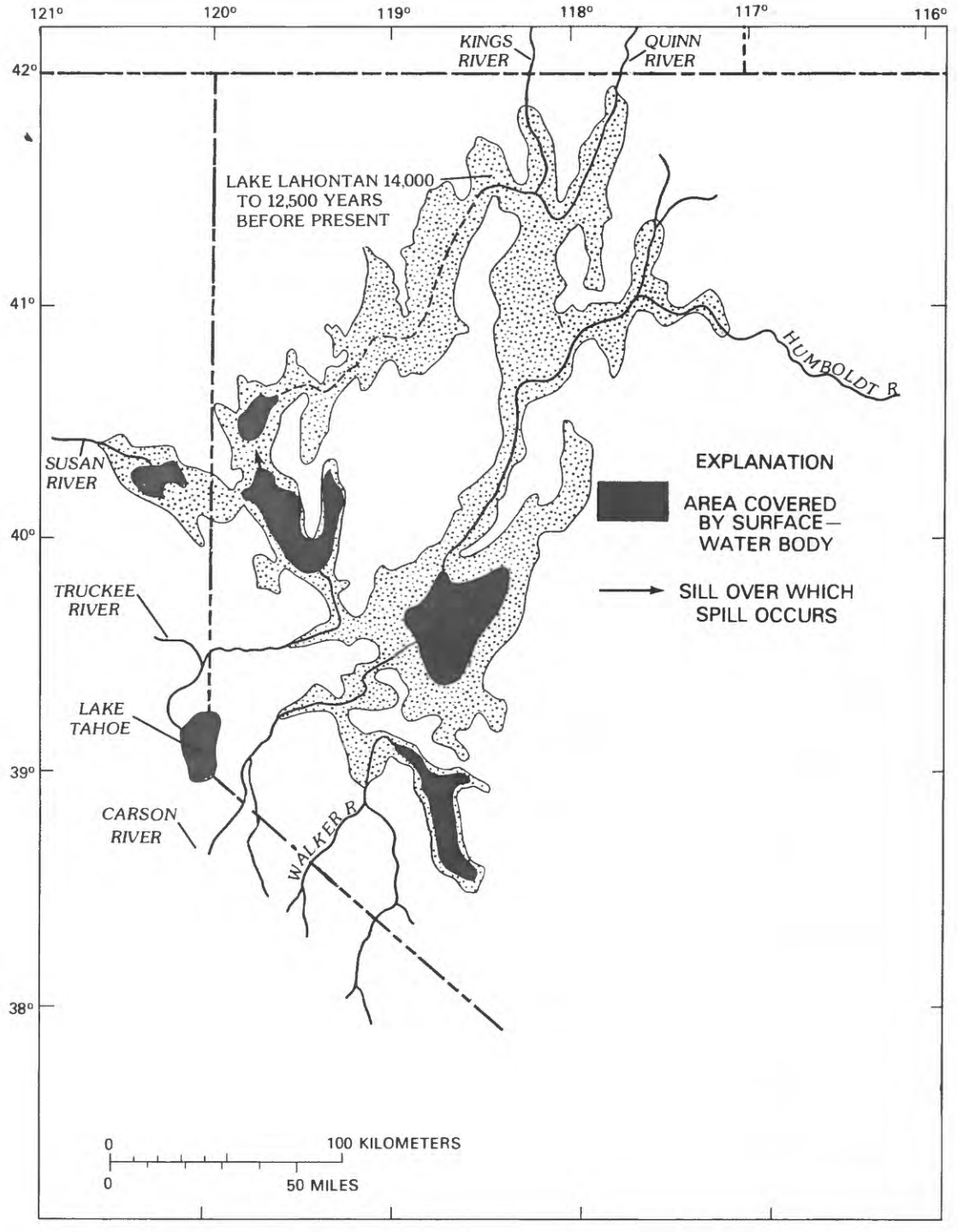

Figure 6.--Hypothetical surface areas of lakes in the Lahontan basin if the runoff and precipitation that occurred in 1969 became the mean.

Turbulence consists of individual eddies having the same function in turbulent transfer that individual molecules have in molecular transfer. These eddies are responsible for the vertical transfer of heat and water vapor. In practice, the evaporation flux, E_v, is determined by measuring the fluctuations, w' and q'.

Aerodynamic (Mass-Transfer) Method

The bulk-aerodynamic equation is expressed as (Quinn, 1979):

$$E=\rho_a C_e (q_o-q)u \tag{3}$$

where E is evaporation rate,

ρ_a is air density,

C_e is bulk-evaporation coefficient,

q_o is saturation-specific humidity at water-surface temperature,

q is specific humidity, and

u is wind velocity.

Quinn (1979) showed that the bulk-aerodynamic equation is similar to the classic mass-transfer equation (U.S. Geological Survey, 1954):

$$E=C_m (e_o-e_a)u \tag{4}$$

where C_m is mass-transfer coefficient,

e_o is saturated vapor pressure at the water-surface temperature, and

e_a is vapor pressure of ambient air.

In both equations, evaporation is considered proportional to wind speed and vapor-pressure (humidity) difference. The coefficient of proportionality represents a combination of many variables, such as size of the lake, roughness of the water surface, kinematic viscosity of the air, and manner of variation of wind speed with height (Harbeck, 1962).

The Dalton Concept

Brutsaert (1984) recently discussed Dalton's (1802) contribution to the development of evaporation theory. Dalton recognized the state of evaporation is increased by: (1) Increasing water-surface temperature; (2) increasing wind speed; and (3) decreasing humidity of ambient air.

Dalton's concept in equation form is:

$$E=f(u)(e_o-e_a) \tag{5}$$

where f(u) is a function of wind velocity, u.

The application of equation (5) to lake evaporation generally involves a wind-speed function of the form (Stelling, 1882):

$$f(u)=a(1+bu) \tag{6a}$$

or

$$f(u)=au \tag{6b}$$

where a and b are empirical constants.

The aerodynamic, mass-transfer, and Dalton-type equations are similar in that evaporation is expressed explicitly as a function of wind speed and the vertical gradient of vapor pressure (or humidity). Evaporation is implicitly a function of water temperature and vapor pressure, in that e_o is calculated using the temperature of the water surface (T_o), and q is calculated, in part, using the temperature of ambient air (T_a). The equations also are similar in that the unexplained physics of the evaporation process is lumped in the value of empirical constants (C_E, C_m, a, b) that multiply the $(e_o-e_a)u$ term.

Energy-Balance Method

Evaporation can be considered as the link between the hydrologic balance, and the energy balance for any surface-water system. A change in the heat stored in a reservoir or lake is the result of heat gains from radiation and advective processes, coupled with heat losses occurring as the result of evaporation. In equation form, this balance can be expressed as:

$$Q_v=R_n+Q_v-Q_e-Q_h-Q_w \tag{7}$$

where Q_v is change in stored-energy content of the water body,

R_n is net-radiative flux density at water surface,

Q_v is heat flux advected by surface- and ground-water sources,

Q_e is latent-heat flux in evaporating water,

Q_h is sensible-heat flux, and

Q_w is the heat flux advected by evaporating water.

Net radiation, R_n, can be divided into several components:

$$R_n=Q_s(1-R_s)+Q_a(1-R_a)-Q_{bs} \tag{8}$$

where Q_s is solar short-wave radiation incident to water surface,

R_s is reflectivity of water surface to short-wave radiation,

Q_a is long-wave radiation incident to water surface,

R_a is reflectivity of water surface to long-wave radiation, and

Q_{bs} is long-wave radiation emitted by water surface.

To write the energy balance in terms of evaporation, the following relations are used:

$$Q_e=\rho_e EL, \tag{9}$$

$$Q_w=\rho_e EC_w(T_o-T_b), \text{ and} \tag{10}$$

$$Q_h=\beta Q_e, \tag{11}$$

where ρ_e is density of water undergoing evaporation,

L is latent heat of vaporization of water,

C_w is specific heat of water,

T_o is surface temperature of water undergoing evaporation,

T_b is an arbitrary base temperature, and

β is the Bowen (1926) ratio

such that

$$E=\frac{Q_s+Q_a+Q_v-(Q_r+Q_{ar}+Q_{bs}+\Delta Q_v)}{\rho_e[L(1+\beta)+C_w(T_o-T_b)]} \tag{12}$$

where $Q_r=R_sQ_s$, short-wave radiation reflected by water surface; and

$Q_{ar}=R_aQ_a$, long-wave radiation reflected by water surface.

The components of equation 12 can be obtained by measurement, or by a parameterization of each component in terms of a combination of theoretical and empirical formulae (for example, U.S. Geological Survey, 1954; Houghton, 1954; U.S. Geological Survey, 1958; Reitan, 1963; Kasten, 1966; Davies and others, 1975; and Berger, 1978). By using the theoretical and empirical formulae, the rate of evaporation can be estimated from values of six measurable climate parameters: (1) Amount of sky cover, (2) type of sky cover, (3) air temperature, (4) water temperature, (5) dew-point temperature (or humidity), and (6) solar irradiation incident on the upper atmosphere.

Combination Methods

This description usually is given to a group of semiempirical methods derived from a combination of energy-balance and Dalton-like approaches. One of the most widely used combination equations is that derived by Penman (1948):

$$E=\frac{\Delta}{\Delta+\gamma}\tilde{Q}_n\pm\frac{\gamma}{\Delta+\gamma}E_A \tag{13}$$

where Δ is slope of the saturation-water vapor-pressure curve at air temperature, T_a;

γ is psychrometric constant; and

$\tilde{Q}_n$ is available energy-flux density divided by latent heat of vaporization.

The E_A term is of the form:

$$E_A=f(u)(e_s-e_a) \tag{14}$$

where e_s is the vapor pressure of saturated air at ambient air temperature; and f(u) (wind function) generally has been formulated in terms of a Stelling-type equation (eq. 6a).

In his derivation, Penman (1948) assummed that the advection (Q_v) and storage (ΔQ_v) terms of the energy-balance equation (eq. 9) were negligible. He also made the assumption that the saturation vapor-pressure curve varied linearly with temperature between the temperature of the water surface, T_o, and the temperature of the air at the level of measurement, T_a,:

$$\left(\frac{de_s}{dT}\right)_{T=T_a} = \frac{e_o-e_s}{T_o-T_a}. \tag{15}$$

One advantage of the Penman equation is that it only requires measurement of humidity, wind speed, and temperature at one level. Another advantage is that it can be used with standard climatological data.

Slatyer and McIlroy (1967) suggested that the first term of equation 13 represented a lower limit to evaporation. They reasoned that, when air has been in contact with a wet surface over a long distance, it will become vapor-saturated, and the value of E_A in the second term of equation 13 will tend to be zero, such that:

$$E=\frac{\Delta\tilde{Q}_n}{\Delta+\gamma}. \tag{16}$$

Priestly and Taylor (1972) used equation 16 as the basis of an empirical relation for evaporation from a wet surface under assumed conditions of vapor saturation. They determined that for large water surfaces, presumably free from advective processes that would tend to reset the vapor-pressure deficit, equilibrium was best described by:

$$E=\Omega\,\frac{(\Delta Q_n)}{(\Delta+\gamma)} \tag{17}$$

where values of Ω usually range from 1.26 to 1.28. Brutsaert (1984) noted this implies, over large wet surfaces, large-scale advection processes still account for 21 to 22 percent of evaporation.

Empirical Methods

A large number of empirical methods have been developed for the estimation of evaporation from water surfaces using commonly measured meteorological parameters, such as humidity or air temperature. In terms of paleoclimate application, a number of authors (Leopold, 1951; Antevs, 1952; Broecker and Orr, 1958; Snyder and Langbein, 1962; Galloway, 1970; Reeves, 1973; Brakenridge, 1978; and Mifflin and Wheat, 1979) have attempted to estimate the evaporation and precipitation responsible for the maintenance of various paleolake systems of probable late-Wisconsin age. The empirical-estimation method used by these authors to estimate evaporation rate can be generalized to include the following steps.

(1) Some indicator of the location of past snowline or timberline (cirque-excavation features, relict-cryogenic deposits, or nivation hollows) was used to estimate the amount of snowline (or timberline) depression relative to the location of modern snowline (or timberline)

(2) Location of the modern snowline was correlated with some mean-seasonal value of temperature (the summer 0 °C, the July 0 °C, or the -6 °C annual isotherm).

(3) A constant-value temperature lapse rate, based sometimes on ground-level meteorological data and other times on free-air radiosonde data, was used to estimate the air-temperature decrease associated with snowline depression.

(4) The same air-temperature decrease in the high-altitude part of the drainage basin also was assumed to have occurred at the altitude of the lake.

(5) The mean-monthly air-temperature decrease usually was distributed within the calendar year either by imposing a graduated decrease of mean-monthly temperature, with the maximum decrease in July and no decrease in January, or by imposing a uniform decrease in monthly air temperature.

(6) A correlation between values of mean-annual or mean-monthly air temperature (at lake-surface altitude) and lake-evaporation rate was attempted and applied to the paleolake system (see, for example, fig. 7).

Early development and application of these empirical procedures for the estimation of evaporation by certain authors (especially Leopold, 1951, and Snyder and Langbein, 1962) stimulated consideration of the climatic conditions responsible for paleolake highstands. The shortcomings of the method and the assumptions on which it was based were recognized and clearly stated in both of these seminal papers. Unfortunately, authors of subsequent papers generally have left unexamined the assumptions underlying the general method outlined before. The assumptions are examined in the following section.

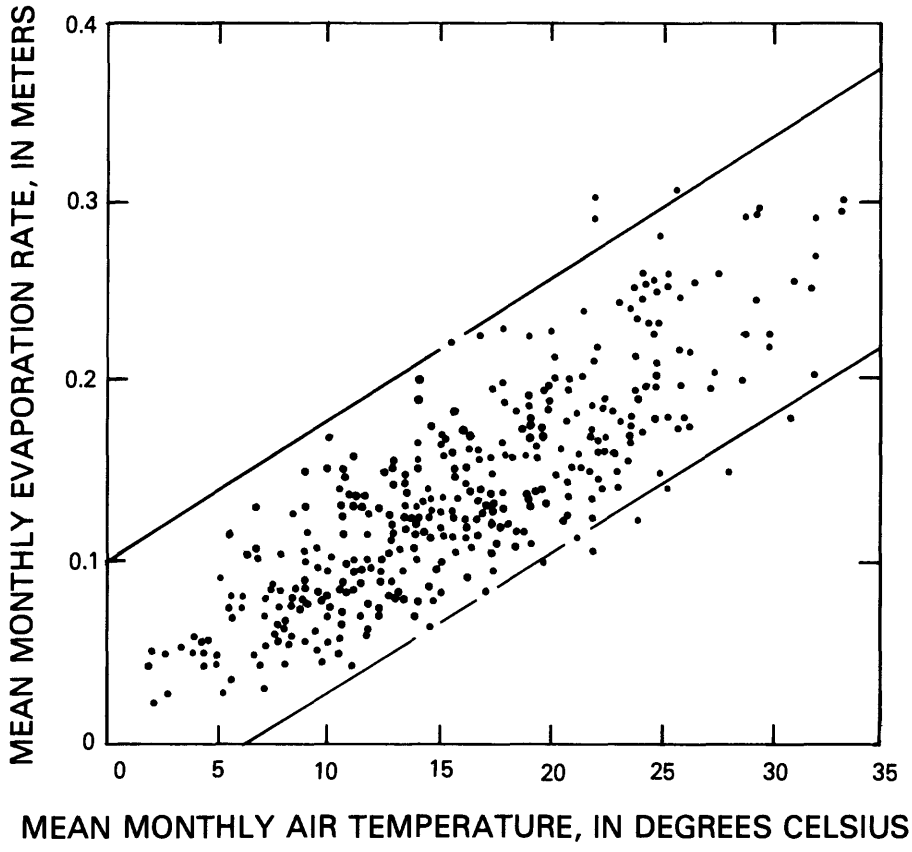

Figure 7.--Relation of evaporation and temperature in the western United States (modified from Galloway, 1970).

Assumption 1: The time of maximum snowline depression is coincident with the time of highest lake stand.

Highstands of large lake systems located in the western United States between 38° and 42° N latitude lag the last continental glacial maximum by periods ranging from 1,000 to 4,000 years (fig. 2). Few data exist on the timing of montane glaciation and deglaciation. Therefore, temperature estimates for times of snowline depression are not necessarily applicable to times of high lake level.

Assumption 2: Free-air and ground-level lapse rates are identical.

Dohrenwend (1984) recently reported that free-air lapse rates are not representative of temperature variation with altitude measured at ground level.

Assumption 3: Temperature-lapse rates are constant in time and space.

Dohrenwend (1984) suggested the following generalized model of temperature variation with altitude, based on empirical data from eight mountain areas in the western United States and on the work of Houghton and others (1975): Below 300 m above basin floors, mean annual lapse rates are approximately zero; above 300 m, mean annual lapse rates are -0.057 °K/100 m for altitudes below 2,000 m and -0.76 °K/100 m for altitudes above 2,000 m. Dohrenwend (1984) suggested that the lapse rate changed with altitude and was not a constant, as assumed by previous workers.

However, even this lapse-rate model need not apply to times of high lake level and mountain glaciation. During such times, temperature at high altitudes would be affected by the nearby mass of glacial ice, and temperature above the lake would be affected by the mass (heat content) of water stored in the lake; that is, both the highstand lake and the mountain glacier represent boundary conditions that "buffer" the lapse rate in their immediate vicinity. Therefore, any quantitative extrapolation of snowline air-temperature estimates to the surface air mass located immediately above lakes situated on distant basin floors seems tenuous.

Assumption 4: Evaporation is solely a function of air temperature.

That this assumption is incorrect is shown in figure 7, which shows that for any mean monthly air temperature, the range of measured evaporation rates about the mean at any particular time is about 0.12 m. This magnitude of scatter is not unexpected, as the review of methods used to calculate present-day evaporation rates indicates that lake evaporation is a function not only of air temperature, but also of water temperature, humidity, cloudiness, and change in heat stored in the lake.

Comparison of Methods and Choice of Energy-Balance Method for the Calculation of Evaporation Rate for Use in Sensitivity Analyses

In terms of calculating the sensitivity of evaporation rate to variation in one or more commonly measured climate parameters, the energy-balance method appears the most promising. Each of the heat terms contained within the energy-balance equation has been shown to have a theoretical or empirical relation to one or more commonly measured climate parameters. The method theoretically is sound and, when applied to computational periods greater than 1 week, has resulted in estimates of evaporation rate nearly the same as those obtained from water-budget calculations (U.S. Geological Survey, 1954). Historically, the energy-balance method has been the standard to which other evaporation methods have been compared.

The covariance method is of little use in studies of past climates because evaporation rate is not treated in terms of commonly measured climate parameters (eq. 2). Mass-transfer and aerodynamic equations of the form presented in this paper (eq. 3 and 4) contain coefficients of proportionality that also vary with lake size and atmospheric stability. Unfortunately, no way exists of predicting the way the form of the wind function varied with past changes in lake size and climate. The Dalton and combination equations

are similar in that they contain a wind function (eq. 5, 6a, and 6b) whose form changes with lake size and atmospheric stability. Empirical methods are based on incorrect assumptions, and evaporation rates calculated using them have been determined to be substantially inaccurate. For these reasons, the energy-balance method was chosen for use in the sensitivity analysis.

THEORETICAL AND EMPIRICAL FORMULAE USED IN THE ENERGY-BALANCE METHOD

Solar Radiation

The sun behaves like a black body with a surface temperature of about 6,000 °K. Most of the emitted radiation is within the shortwave band between 0.3 and 3.0 μm. The shortwave irradiation at the upper atmosphere of the Earth, normal to the solar beam, is known as the Solar Constant and has a value of about 1.94 cal cm^{-2} min^{-1}. The irradiation is not truly constant; it changes as the Earth's orbit varies in response to lunar and planetary gravitational perturbations (fig. 8).

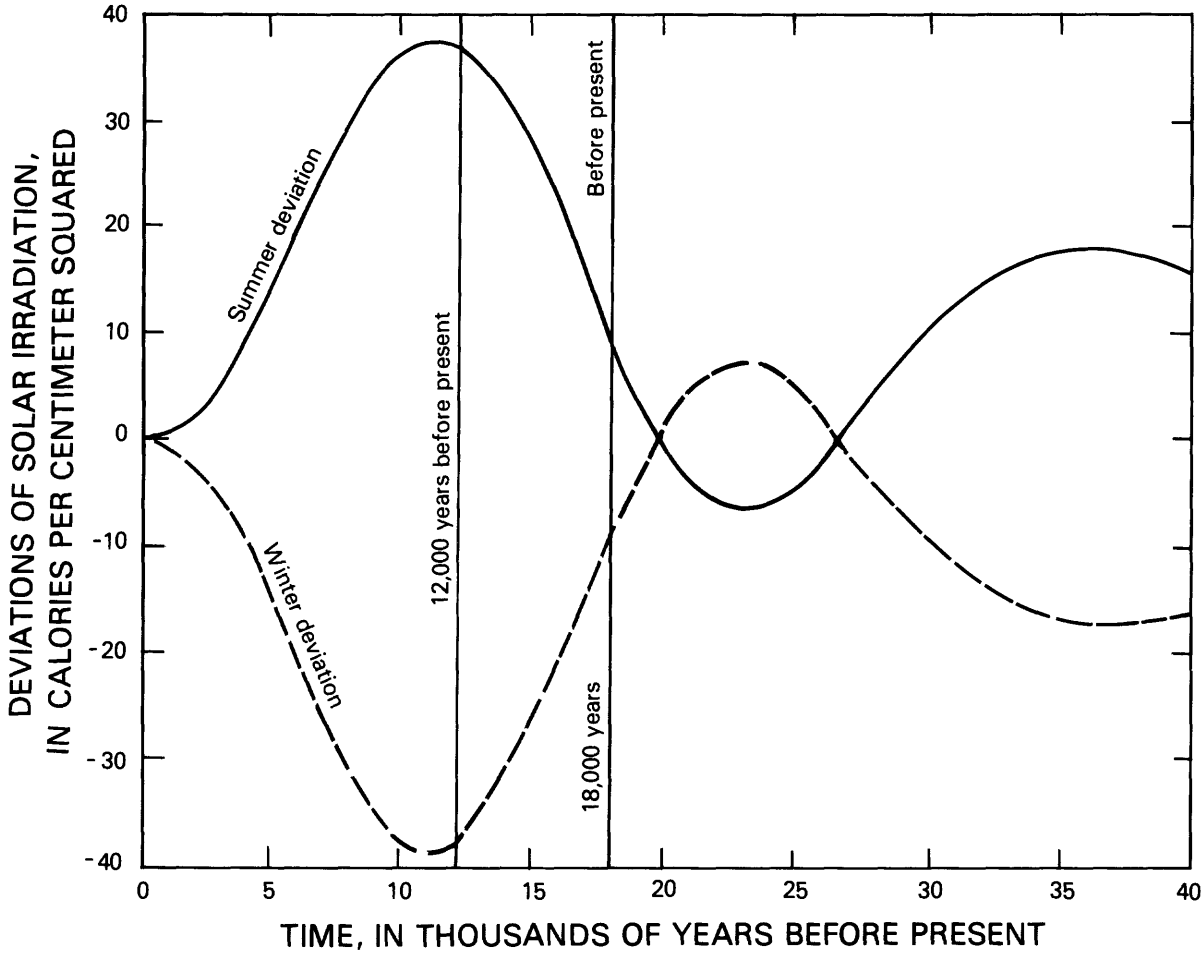

Figure 8.--Deviations of solar irradiation from their 1950 values at 40° north latitude.

Short-wave Radiation

As it passes through the atmosphere, solar radiation is modified by scattering, absorption, and reflection by particles and molecules. The proportion of solar radiation that reaches the Earth's surface may be calculated with the use of atmospheric-transmission coefficients that relate the attenuation of solar radiation to scattering, absorption, and reflection processes:

$$Q_s = Q^* \tau_{da} \tau_{ws} \tau_{wa} \tau_{ab} \quad (18)$$

where Q_s is solar radiation incident to land surface,

Q^* is solar irradiation incident on the upper atmosphere,

τ_{da} is atmospheric-transmission coefficient resulting from dry-air scattering,

τ_{ws} is atmospheric-transmission coefficient resulting from water-vapor scattering,

τ_{wa} is atmospheric-transmission coefficient resulting from absorption by water vapor, and

τ_{ab} is atmospheric-transmission coefficient resulting from reflection (albedo) by clouds.

The solar irradiation (insolation) at any given latitude on the Earth is a single-valued function of the solar constant, the semimajor axis of the Earth's orbit, its eccentricity, the obliquity, and the longitude of the perihelion measured from the moving vernal equinox. Values of solar irradiation were obtained from Berger (1978).

Equations for calculation of atmospheric-transmission coefficients are given in Davies and others (1975):

$$\tau_{da} = 0.972 - 0.8262\bar{M} + 0.00933\bar{M}^2 - 0.00095\bar{M}^3 + 0.0000437\bar{M}^4 \quad (19)$$

$$\tau_{ws} = 1 - 0.0225W\bar{M}, \text{ and} \quad (20)$$

$$\tau_{wa} = 1 - 0.007(W\bar{M})^{0.3}. \quad (21)$$

W, the precipitable water vapor aloft, can be related to measured surface dew-point temperature (T_{dp}) through an equation formulated by Reitan (1963):

$$W = \exp[0.1102 + (0.06138(T_{dp} - 273.15))]; \quad (22)$$

and the mean optical air mass ($\bar{M}$); that is, the depth of atmosphere traversed by the solar beam. $\bar{M}$ can be approximated with an equation formulated by Kasten (1966):

$$M = 1/[\sin(90^\circ - \bar{Z}) + 0.150(90^\circ - \bar{Z} + 3.885)^{-1.253}] \quad (23)$$

in which the mean zenith angle ($\bar{Z}$) can be calculated using

$$\cos\bar{Z} = Q^*/[(S\bar{d}/d)^2(60\bar{t})] \quad (24)$$

where S is solar constant,
$\bar{d}/d$ is ratio of the mean Earth-sun distance to instantaneous distance, and
$\bar{t}$ is duration of sunshine at any specific latitude.

Sunshine durations are tabulated in List (1951) and also can be calculated using an algorithm derived by Swift (1976).

The atmospheric-transmission coefficient resulting from cloud albedo can be calculated from:

$$\tau_{ab}=1-(A_{hl}f_{hl}\chi+A_{ml}f_{ml}\chi+A_{ll}f_{ll}\chi) \tag{25}$$

where A_{hl} is albedo of high-altitude cirrus clouds,
A_{ml} is albedo of medium-altitude clouds,
A_{ll} is albedo of low-level heap clouds,
f_{hl} is fraction of sky covered by high-altitude clouds,
f_{ll} is fraction of sky covered by low-altitude clouds,
f_{ml} is fraction of sky covered by medium-altitude clouds, and
χ is total fraction of sky covered by clouds.

Houghton (1954) recommends cloud-albedo values of $A_{hl}=0.21$, $A_{ml}=0.48$, and $A_{ll}=0.70$.

A part of the solar radiation reaching a water surface also is reflected by that surface:

$$Q_r=R_sQ_s \tag{26}$$

where Q_r is the part of incoming solar radiation that is reflected from water surface, and
R_s is solar-radiation reflectivity of the water surface.

Houghton (1954) recommends the use of a value of 0.07 for R_s.

Long-Wave Radiation

Long-wave radiation is absorbed and emitted mainly by water vapor, carbon dioxide, and ozone, to a lesser extent. Long-wave radiation incident to a water surface can be approximated by empirical formulae relating radiation to cloud height, cloud amount, and ambient vapor pressure (U.S. Geological Survey, 1954):

$$Q_a=Q_{a,hl}+Q_{a,ml}+Q_{a,ll}, \tag{27}$$

$$Q_{a,hl}=f_{hl}\sigma T_a^4(a_{hl}+b_{hl}e_a), \tag{28}$$

$$Q_{a,ml}=f_{ml}\sigma T_a^4(a_{ml}+b_{ml}e_a), \text{ and} \tag{29}$$

$$Q_{a,ll}=f_{ll}\sigma T_a^4(a_{ll}+b_{ll}e_a), \tag{30}$$

where $Q_{a,hl}$ is long-wave radiation falling on water surface from high-level clouds,

$Q_{a,ml}$ is long-wave radiation falling on water surface from medium-level clouds,

$Q_{a,ll}$ is long-wave radiation falling on water surface from low-level clouds, and

σ is Stefan's constant ($\sigma = 11.71 \times 10^{-8}$ cal cm^2 d^{-1} °K^{-1} day).

Additional parameterizations used in equations 28-30 are:

$$a_{hl}=0.74+f_{hl}(0.025\chi e^{-0.1916\alpha_{hl}}), \tag{31}$$

$$a_{ml}=0.74+f_{ml}(0.025\chi e^{-0.1916\alpha_{ml}}), \tag{32}$$

$$a_{ll}=0.74+f_{ll}(0.025\chi e^{-0.1916\alpha_{ll}}), \tag{33}$$

$$b_{hl}=0.00490-f_{hl}(0.00054\chi e^{-0.1969\alpha_{hl}}), \tag{34}$$

$$b_{ml}=0.00490-f_{ml}(0.00054\chi e^{-0.1969\alpha_{ml}}), \text{ and} \tag{35}$$

$$b_{ll}=0.00490-f_{ll}(0.00054\chi e^{-0.1969\alpha_{ll}}), \tag{36}$$

where α_{hl} is altitude of high-level clouds (6 km),

α_{ll} is altitude of low-level clouds (1 km), and

α_{ml} is altitude of medium-level clouds (4 km).

Part of the long-wave radiation reaching the water surface is reflected:

$$Q_{ar}=R_a Q_a \tag{37}$$

where R_a is long-wave reflectivity of water surface; Houghton (1954) recommends a value of 0.03 for R_a, and

Q_{ar} is the part of incoming long-wave radiation that is reflected from water surface back to atmosphere.

Part of the long-wave radiation absorbed by the body of water is emitted to the atmosphere:

$$Q_{bs}=\sigma T_o^4 \tilde{e} \tag{38}$$

where $\tilde{e}$, the emissivity of water, equals 0.970±0.005 (U.S. Geological Survey, 1954).

During the process of evaporation, heat is transferred to the atmosphere as latent heat (Q_e), sensible heat (Q_h), and advected heat (Q_w). These heat fluxes can be calculated from:

$$Q_e=\rho_e EL, \text{ and}$$

$$Q_w=\rho_e C_w E(T_o-T_b).$$

Because the atmospheric-transport mechanisms of sensible heat and water vapor are similar, the sensible-heat flux generally is treated with the rate of evaporation. The ratio of these fluxes is called the Bowen ratio, β:

$$\beta=\frac{Q_h}{Q_e}$$

which, combined with equation 9, yields:

$$\beta=\frac{Q_h}{\rho_e EL}. \tag{39}$$

Bowen (1926) determined that if water vapor and sensible-heat transport both were expressed in the form of a diffusion equation, the Bowen ratio, β, would be written in terms of temperature and vapor pressure gradients; that is:

$$\beta=\gamma\frac{T_o-T_a}{e_o-e_a}; \tag{40}$$

where γ, the psychrometric constant, is given by

$$\gamma=\frac{c_p P}{0.622L} \tag{41}$$

and where P is the ambient air pressure, in millibars, and c_p is the specific heat of air at constant pressure.

Heat reaching the water body by advection (streamflow and overland runoff, ground-water discharge, and precipitation directly onto the water body) can be calculated from a knowledge of the volumes of advected fluids, their temperatures, and their heat capacities:

$$Q_v=\sum_{i=1}^{n}\rho_v V_i(\bar{T}_i-T_b)C_w \tag{42}$$

where ρ_v is density of advected water,

V_i is volume of the ith source of advected water integrated over any convenient time, and

$\bar{T}_i$ is mean temperature of the ith source of advected water averaged over the time used to calculate V_i.

A change in the heat stored in the water body can occur as the result of the sum of the individual heat-transfer processes. The stored heat can be calculated from a knowledge of the mean temperature, heat capacity, and volume of the body of water. This calculation usually is made by vertically subdividing the body of water into a number of layers of equal thickness. The heat content of each layer is calculated, and the heat contents of all layers are summed:

$$Q_v = \sum_{j=1}^{k} \rho_j C_w (\overline{T}_j - T_b) \Delta x_j A_j \qquad (43)$$

where ρ_j is density of the jth layer of water,

$\overline{T}_j$ is mean temperature of the jth layer of water,

Δx_j is thickness of each layer of water, and

A_j is area of the jth layer of water.

In certain situations, the time over which the energy balance is calculated can be chosen so that $\Delta Q_v = 0$. For example, the balance can be made over a time starting and ending with the lake in the same isothermal state. For certain situations, the advection heat term, Q_v, also can be ignored. For example, the temperature of much of the runoff from the Sierra Nevada is near 0 °C (the base temperature in our computations); therefore, the heat transported by such streams tends to be small in comparison to the other heat terms in the energy-balance equation. Finally, the heat-balance calculation can be carried out over a time for which the addition of advected heat is equivalent to the increase of stored heat, such that:

$$\Delta Q_v - Q_v = 0. \qquad (44)$$

Having established theoretical and empirical relations for components of the energy balance (eq. 9 and 10) in terms of measurable climate parameters (eqs. 11 through 43), the sensitivity of evaporation rate to changes in each of six climate parameters--(1) amount and (2) type of sky cover, (3) air temperature, (4) water temperature, (5) dew-point temperature (or humidity), and (6) solar irradiation incident on the upper atmosphere--now can be determined.

SENSITIVITY ANALYSIS

For the sensitivity analysis, a reference lake-climate system first needs to be established. The lake chosen as a reference site was Pyramid Lake, Nev. (fig. 1 and table 3). The reference lake-climate system was a composite of land-based mean monthly meteorological data recorded at the Reno, Nev., weather station (U.S. Weather Bureau, 1950-65; National Oceanic and Atmospheric Administration, 1966-75) and lake-based water-surface temperature measurements made at Pyramid Lake during 1976 and 1977 (Benson, 1984). The reference sky was assumed to be composed of 80-percent high-level clouds,

10-percent medium-level clouds, and 10-percent low-level clouds. A computer program (EVAP, table 4) was used to calculate evaporation rate in terms of the empirical and theoretical relations previously established between the climatic parameters of the reference data set and the heat terms contained in equation 12. The calculated evaporation rate of 1.10 m yr^{-1} (table 5) was in reasonable agreement with mean annual evaporation rate of 1.2±0.1 m, determined by Harding (1965) for 1932-52, using a water-budget method. However, the agreement between the results of the energy-balance and water-budget methods resulted from use of meteorological data recorded at a land-based site located 60 km south of the center of Pyramid Lake. The temperature and relative humidity of air at some standard distance over the land-based site will not be the same over the lake surface. Therefore the agreement between calculated and measured rates of evaporation may be fortuitous.

Table 3.--*Reference-climate data set for Pyramid Lake, Nevada*

[°K, degrees Kelvin; mb, millibars; cal cm^{-2} day^{-1}, calories per centimeter squared per day]

Month	Air temperature (°K)	Water temperature (°K)	Sky cover (fraction)	Pressure (mb)	Optical air mass	Solar irradiation (cal cm^{-2} day^{-1})	Dew-point temperature (°K)
January----	273.0	279.7	0.65	866	2.99	374	267.4
February---	276.4	279.7	.61	865	2.57	513	269.6
March------	278.2	279.7	.58	863	2.11	690	269.1
April------	281.2	282.2	.55	863	1.90	852	270.6
May--------	285.8	285.2	.48	863	1.81	961	274.2
June-------	290.0	289.7	.35	863	1.70	996	277.3
July-------	294.2	294.2	.22	865	1.78	954	279.4
August-----	293.0	294.2	.21	864	1.84	842	279.0
September--	288.6	293.2	.23	864	2.01	680	276.7
October----	283.6	290.7	.39	865	2.36	507	273.9
November---	277.6	287.2	.57	866	2.83	372	270.7
December---	273.6	283.2	.63	866	3.16	322	268.4

Table 4.--EVAP computer program listing

[Abbreviations in table are included in symbols, variables, dimensions, and definitions list at the beginning of manuscript]

```
      REAL SKY(12),HUMID(12),WLOFT(12),AIRT(12),WATERT(12),TAUDRY(12)
      REAL TAUSCAT(12),TAUWET(12),P(12),NUM(12),DENOM(12),DEWPT(12)
      REAL TAUALB(12),MASSAIR(12),QS(12),QSTAR(12),SVPDEW(12)
      REAL SVP2M(12),QA(12),QR(12),Q4R(12),SVPOM(12)
      REAL BOWRAT(12),QBS(12),LHEAT(12),MEVAP(12),ANEVAP
      REAL AH(12),AM(12),AL(12),BH(12),BM(12),BL(12),ARWATR(12)
      REAL ALBHI,ALBMED,ALBLO,ALTHI,ALTMED,ALTLO,D0,D1,D2,D3,D4,D5,D6
      REAL BASET,FRLO(10),FRHI(10),FRMED(10)
      REAL QV(12),QNU(12),QAH(12),QAM(12),QAL(12)
      REAL SUMARY(20,10),HI(20,10),MED(20,10),LOW(20,10)



      CHARACTER * 30 TITLE
      INTEGER I,LHEAD,J

      OPEN (5,FILE = 'WORK.IN')
      OPEN (6,FILE = 'WORK.OUT')
      OPEN (7,FILE = 'SUMMARY')

      READ(5,102)(FRHI(I),I=1,10)
      READ(5,102)(FRMED(I),I=1,10)
      READ(5,102)(FRLO(I),I=1,10)

          DO 1500 J=1,20

      READ (5,100) TITLE
      IF (TITLE.EQ.'QUIT'.OR.TITLE.EQ.'quit') GO TO 8
      READ (5,101) (SKY(I),I=1,12)
      READ (5,101)(DEWPT(I),I=1,12)
      READ (5,101)(AIRT(I),I=1,12)
      READ (5,101)(WATERT(I),I=1,12)
      READ (5,*)(QSTAR(I),I=1,12)
      READ (5,101)(MASSAIR(I),I=1,12)
      READ (5,101)(P(I),I=1,12)
      READ (5,101)(QV(I),I=1,12)
      READ (5,101)(QNU(I),I=1,12)

C     CONSTANTS

      ALBHI=.21
      ALBMED=.48
      ALBLO=.70
      ALTHI=6.0
      ALTMED=4.0
      ALTLO=1.0
      D0=6984.505294
      D1=-188.9039310
      D2=2.133357675
      D3=-1.288580973E-2
      D4=4.393587233E-5
      D5=-8.023923082E-8
      D6=6.136820929E-11
```

Table 4.--EVAP computer program listing--Continued

```
      BASET=273.15

      WRITE(6,899)
      N=0
      DO 1100 K=1,10

           WRITE(6,98) TITLE

             HI(J,K)=FRHI(K)*100.
             MED(J,K)=FRMED(K)*100.
             LOW(J,K)=FRLO(K)*100.
                      WRITE(6,702) HI(J,K)
                      WRITE(6,703) MED(J,K)
                      WRITE(6,704) LOW(J,K)
             WRITE (6,490)
           ANEVAP=0

           DO 1000 I=1,12


                WLOFT(I)=EXP((.1102 + .06138*(DEWPT(I)-273.15)))
                TAUSCAT(I)=1-(0.0225*WLOFT(I)*MASSAIR(I))
                TAUDRY(I)=0.972-(0.09262*MASSAIR(I))+0.00933*
C                      (MASSAIR(I)**2)-0.00095*(MASSAIR(I)**3)+
C                      0.0000437*(MASSAIR(I)**4)
                TAUWET(I)=1-(0.077*((WLOFT(I)*MASSAIR(I))**.3))
                TAUALB(I)=1-((ALBHI*FRHI(K)*SKY(I))+(ALBMED*FRMED(K)*
C                      SKY(I))+(ALBLO*FRLO(K)*SKY(I)))
                QS(I)=QSTAR(I)*TAUDRY(I)*TAUSCAT(I)*TAUWET(I)*TAUALB(I)
                QR(I)=.07*QS(I)
                AM(I)=.74+FRMED(K)*(.025*SKY(I)*EXP(-0.1916*ALTMED))
                BM(I)=0.0049-(0.0054*SKY(I)*EXP(-0.1969*ALTMED))*FRMED(K)
                AH(I)=.74+FRHI(K)*(.025*SKY(I)*EXP(-0.1916*ALTHI))
                AL(I)=.74+FRLO(K)*(.025*SKY(I)*EXP(-0.1916*ALTLO))
                BH(I)=0.0049-(0.0054*SKY(I)*EXP(-0.1969*ALTHI))*FRHI(K)
                BL(I)=0.0049-(0.0054*SKY(I)*EXP(-0.1969*ALTLO))*FRLO(K)
                SVP2M(I)=D0+AIRT(I)*(D1+AIRT(I)*(D2+AIRT(I)*(D3+AIRT(I)*
C                      (D4+AIRT(I)*(D5+D6*AIRT(I))))))
                SVPDEW(I)=D0 +DEWPT(I)*(D1+DEWPT(I)*(D2+DEWPT(I)*(D3+
C                      DEWPT(I)*(D4+DEWPT(I)*(D5+D6*DEWPT(I))))))
                HUMID(I)=SVPDEW(I) / SVP2M(I)

                QAH(I)=FRHI(K) * (1.171E-07 * AIRT(I)**4)*
C                      (AH(I)+ BH(I)* SVPDEW(I))
                QAM(I)=FRMED(K) * (1.171E-07 * AIRT(I)**4)*
C                      (AM(I)+ BM(I)* SVPDEW(I))
                QAL(I)=FRLO(K) * (1.171E-07 * AIRT(I)**4)*
C                      (AL(I)+ BL(I)* SVPDEW(I))
                QA(I)=QAH(I)+QAM(I)+QAL(I)
                QAR(I)=0.0301*QA(I)
                QBS(I)=1.171E-07*(WATERT(I)**4)*0.97
                LHEAT(I)=(-0.57*WATERT(I))+753.1
                SVPOM(I)=D0+WATERT(I)*(D1+WATERT(I)*(D2+WATERT(I)*
C                      (D3+WATERT(I)*(D4+WATERT(I)*(D5+D6*WATERT(I))))))
                BOWRAT(I)=0.61*(WATERT(I)-AIRT(I))/((SVPOM(I)-SVPDEW(I))*
```

Table 4.--EVAP computer program listing--Continued

```
      C                    (1000/P(I)))
                  NUM(I)=QS(I)+QA(I)+QV(I)-(QR(I)+QAR(I)+QBS(I)+QNU(I))
                  DENOM(I)=(LHEAT(I)*(1+BOWRAT(I)))+(WATERT(I)-BASET)
                  MEVAP(I)=(NUM(I)/DENOM(I))*30.42
                  ANEVAP=MEVAP(I)+ANEVAP
                  ARWATR(I)= WATERT(I) - AIRT(I)
1000          CONTINUE
              ANEVAP=ANEVAP/100
              SUMARY(J,K)=ANEVAP
1111          WRITE(6,900)
              WRITE(6,304)(AIRT(I),I=1,12)
              WRITE(6,305)(WATERT(I),I=1,12)
              WRITE(6,301)(SKY(I),I=1,12)
              WRITE(6,311)(P(I),I=1,12)
              WRITE(6,310)(MASSAIR(I),I=1,12)
              WRITE(6,309)(QSTAR(I),I=1,12)
              WRITE(6,495)(DEWPT(I),I=1,12)
              WRITE(6,490)
              WRITE(6,423)(ARWATR(I),I=1,12)
              WRITE(6,302)(HUMID(I),I=1,12)
              WRITE(6,303)(WLOFT(I),I=1,12)
              WRITE(6,450)(LHEAT(I),I=1,12)
              WRITE(6,306)(TAUDRY(I),I=1,12)
              WRITE(6,307)(TAUSCAT(I),I=1,12)
              WRITE(6,308)(TAUWET(I),I=1,12)
              WRITE(6,411)(TAUALB(I),I=1,12)
              WRITE(6,455)(SVP1M(I),I=1,12)
              WRITE(6,456)(SVP2M(I),I=1,12)
              WRITE(6,457)(SVPDEW(I),I=1,12)
              WRITE(6,412)(QS(I),I=1,12)
              WRITE(6,420)(QR(I),I=1,12)
              WRITE(6,417)(QBS(I),I=1,12)
              WRITE(6,458)(QAH(I),I=1,12)
              WRITE(6,459)(QAM(I),I=1,12)
              WRITE(6,460)(QAL(I),I=1,12)
              WRITE(6,415)(QA(I),I=1,12)
              WRITE(6,416)(QAR(I),I=1,12)
              WRITE(6,461)(QV(I),I=1,12)
              WRITE(6,462)(QNU(I),I=1,12)
              WRITE(6,418)(BOWRAT(I),I=1,12)
              WRITE(6,421)(NUM(I),I=1,12)
              WRITE(6,422)(DENOM(I),I=1,12)
              WRITE(6,490)
              WRITE(6,425)(MEVAP(I),I=1,12)
              WRITE(6,485) ANEVAP
              WRITE(6,399)
1100      CONTINUE

1500      CONTINUE
C         THIS NEXT SECTION IS TO SUMMARIZE THE EVAPORATION RESULTS
C         THE DATA FILE IS CLOSED AND REOPENED FOR THE TITLE

8         CONTINUE

          REWIND(5)
```

Table 4.--EVAP computer program listing--Continued

```
      DO 11 J=1,20
         IF (J .LT. 2)GO TO 94
         READ (5,97,END=999,ERR=999) TITLE
         GO TO 96
94       READ (5,99,END=999,ERR=999) TITLE

96       WRITE(7,899)
       DO 20 K=1,10
         WRITE(7,465)TITLE
         WRITE(7,466)HI(J,K),MED(J,K),LOW(J,K)
         WRITE(7,485)SUMARY(J,K)
20    CONTINUE
11     CONTINUE
98    FORMAT(18X,A80)
97    FORMAT(A80,9(/))
99    FORMAT(3(/),A80,9(/))
100   FORMAT(A80)
101   FORMAT(12F6.2)
102   FORMAT(10F4.3)
103   FORMAT(5F6.2,F7.2,6F6.2)
301   FORMAT(1X,'SKY          ',12F6.2)
302   FORMAT(1X,'HUMID        ',12F6.2)
303   FORMAT(1X,'WLOFT        ',12F6.2)
304   FORMAT(1X,'AIRT         ',12F6.1)
305   FORMAT(1X,'WATERT       ',12F6.1)
306   FORMAT(1X,'TAU  DA      ',12F6.2)
307   FORMAT(1X,'TAU  WS      ',12F6.2)
308   FORMAT(1X,'TAU  WA      ',12F6.2)
309   FORMAT(1X,'QSTAR        ',12F6.0)
310   FORMAT(1X,'MASSAIR      ',12F6.2)
311   FORMAT(1X,'P            ',12F6.0)
411   FORMAT(1X,'TAU AB       ',12F6.2)
412   FORMAT(1X,'QS           ',12F6.0)
415   FORMAT(1X,'QA           ',12F6.0)
416   FORMAT(1X,'QAR          ',12F6.0)
417   FORMAT(1X,'QBS          ',12F6.0)
418   FORMAT(1X,'BOWRAT       ',12F6.3)
420   FORMAT(1X,'QR           ',12F6.0)
421   FORMAT(1X,'NUM          ',12F6.1)
422   FORMAT(1X,'DENOM        ',12F6.0)
423   FORMAT(1X,'WATERT-AIRT  ',12F6.1)
425   FORMAT(1X,'MEVAP        ',12F6.2)
450   FORMAT(1X,'LHEAT        ',12F6.1)
455   FORMAT(1X,'SVPOM        ',12F6.2)
456   FORMAT(1X,'SVP2M        ',12F6.2)
457   FORMAT(1X,'SVPDEW         ',12F6.2)
458   FORMAT(1X,'QAH          ',12F6.0)
459   FORMAT(1X,'QAM          ',12F6.0)
460   FORMAT(1X,'QAL          ',12F6.0)
461   FORMAT(1X,'QV           ',12F6.2)
462   FORMAT(1X,'QNU          ',12F6.2)
465   FORMAT(1H0,3X,A80)
466   FORMAT(1H ,15X,F4.1,'% HI CLOUDS',5X,
     C        F4.1,'% MED CLOUDS',/1H ,25X,F4.1,'% LOW CLOUDS')
485   FORMAT(1H ,20X,'MEAN ANNUAL EVAPORATION =',F8.3,' M/Y')
```

Table 4.--EVAP computer program listing--Continued

```
490     FORMAT(1HO)
495     FORMAT(1X,'DEWPT       ',12F6.1)
702     FORMAT(1H ,30X,F4.1,' PERCENT HI CLOUDS')
703     FORMAT(1H ,30X,F4.1,' PERCENT MEDIUM CLOUDS')
704     FORMAT(1H ,30X,F4.1,' PERCENT LOW CLOUDS')
899     FORMAT (1H1)
900     FORMAT(6X,'       JAN    FEB    MAR    APR    MAY    JUN    JUL    AUG
     +  SEP    OCT    NOV    DEC')

999       ENDFILE (6)
          ENDFILE (7)
        CLOSE (6)
        CLOSE (5)
        CLOSE (7)

9999    STOP
        END
```

Table 5.--*Computed evaporation rates, in meters per year for fractions of cloud type, amount of sky cover, and various combinations of air temperature, water temperature, and relative humidity*

[Values of solar irradiation are for 12,000 years before present, unless otherwise noted. f_{hl}, fraction of high-level clouds; f_{ml}, fraction of medium-level clouds; f_{ll}, fraction of low-level clouds; °K, degree Kelvin]

Fractions of cloud type			Increase in amount of sky cover relative to reference data set (table 3)							Variations in air temperature, water temperature, and relative humidity
f_{hl}	f_{ml}	f_{ll}	0 percent	10 percent in January	10 percent in August	20 percent in January	10 percent each month	20 percent in August	20 percent each month	
0.80	0.10	0.10	1.166	1.135	1.124	1.104	1.094	1.083	1.022	Values for air temperature, water temperature, and relative humidity taken from reference data set (table 3).
.70	.20	.10	1.139	1.105	1.094	1.071	1.061	1.049	.983	
.70	.10	.20	1.117	1.081	1.069	1.044	1.033	1.021	.949	
.60	.30	.10	1.112	1.076	1.063	1.039	1.027	1.015	.943	
.60	.20	.20	1.090	1.051	1.038	1.012	1.000	.987	.910	
.50	.40	.10	1.085	1.046	1.032	1.006	.994	.980	.902	
.50	.30	.20	1.063	1.021	1.007	.979	.966	.952	.869	
.50	.20	.30	1.041	.997	.982	.952	.939	.924	.836	
.40	.30	.30	1.014	.967	.951	.919	.905	.889	.796	
.33	.33	.33	.986	.936	.920	.886	.871	.854	.756	
0.80	0.10	0.10	0.753	0.729	0.719	0.706	0.696	0.685	0.639	Values for air temperature reduced 5°K and values for relative humidity increased 20 percent each month relative to reference data set (table 3).
.70	.20	.10	.732	.706	.695	.681	.670	.659	.608	
.70	.10	.20	.715	.688	.675	.660	.649	.636	.582	
.60	.30	.10	.711	.683	.671	.655	.644	.632	.577	
.60	.20	.20	.694	.665	.652	.635	.623	.609	.551	
.50	.40	.10	.690	.660	.647	.630	.618	.604	.545	
.50	.30	.20	.673	.641	.628	.609	.596	.582	.520	
.50	.20	.30	.656	.622	.608	.588	.575	.560	.493	
.40	.30	.30	.635	.599	.584	.563	.549	.533	.462	
.33	.33	.33	.576	.576	.559	.537	.522	.505	.430	
0.80	0.10	0.10	0.639	0.614	0.607	0.589	0.582	0.575	0.526	Values for air temperature reduced 15 °K in July and no reduction in January relative to reference data set (table 3).
.70	.20	.10	.617	.590	.582	.562	.555	.547	.493	
.70	.10	.20	.599	.570	.561	.541	.533	.524	.467	
.60	.30	.10	.595	.565	.557	.535	.528	.519	.460	
.60	.20	.20	.577	.546	.536	.514	.506	.496	.434	
.50	.40	.10	.573	.541	.532	.509	.500	.491	.428	
.50	.30	.20	.555	.521	.512	.487	.478	.468	.401	
.50	.20	.30	.538	.502	.491	.466	.456	.446	.375	
.40	.30	.30	.516	.478	.467	.439	.429	.418	.342	
.33	.33	.33	.494	.453	.442	.413	.402	.390	.310	
0.80	0.10	0.10	0.569	0.547	0.537	0.525	0.516	0.505	0.463	Values for air temperature reduced 10 °K and values for relative humidity increased 10 percent each month relative to reference data set (table 3).
.70	.20	.10	.549	.525	.514	.501	.491	.479	.433	
.70	.10	.20	.533	.507	.495	.482	.471	.459	.409	
.60	.30	.10	.529	.503	.491	.477	.466	.454	.403	
.60	.20	.20	.513	.486	.473	.458	.446	.433	.379	
.50	.40	.10	.509	.482	.468	.453	.441	.428	.373	
.50	.30	.20	.493	.464	.450	.434	.421	.407	.349	
.50	.20	.30	.477	.446	.431	.415	.401	.386	.325	
.40	.30	.30	.458	.424	.409	.391	.376	.361	.295	
.33	.33	.33	.438	.403	.386	.367	.352	.335	.266	

Parameter Variation

Eight parameters: (1) Air temperature (T_a); (2) water temperature (T_o); (3) amount of sky cover (χ); (4) solar irradiation at the upper atmosphere (Q^*); (5) fraction of high-level clouds (f_{hl}); (6) fraction of medium-level clouds (f_{ml}); (7) fraction of low-level clouds (f_{ll}); and (8) dewpoint temperature (T_{dp}) were varied in the sensitivity study. Variations in dewpoint temperatures were adjusted to correspond to simple percentage changes in relative humidity (RH). Dewpoint temperature was varied independently of air and water temperature by adjusting the ambient vapor pressure.

Four types of parameter distributions were employed. In the first type of distribution, the same change or set of conditions was imposed on the monthly reference state. Examples are a decrease of 5 °K in mean monthly air temperature, and a 20-percent increase in the absolute mean monthly sky cover.

The second type of distribution was characterized by a scaled reduction (or increase) in a parameter each month, with the maximum reduction (or increase) in July or August and no reduction in January. Examples are a decrease of 10 °K in the July air temperature, with no reduction in the January air temperature, and a 20-percent increase in August sky cover, with no increase in January sky cover. Mean monthly values for this type of distribution were calculated using an equation of the form:

$$\left[\frac{\Delta X_j}{X_j - X_o}(X_o - X_i) + X_i\right] = X_i + \Delta X_i \tag{45}$$

where X_i is historical mean monthly value for parameter X,

X_j is maximum mean monthly value for parameter X,

X_o is minimum mean monthly value for parameter X,

ΔX_j is maximum reduction (or increase) made to July (or August) value of X, and

$X_i + \Delta X_i$ is scaled value of parameter X for the ith month.

The third type of distribution was characterized by a scaled increase in sky cover each month, with the maximum increase in January and no change in August. Mean monthly values for this distribution were calculated using an equation of the form:

$$\left[\frac{\Delta X_o}{X_o - X_j}(X_o - X_i) + X_i\right] = X_i + \Delta X_i; \tag{46}$$

where all symbols have been previously defined, except ΔX_o, the maximum increase applied to the January value.

The fourth type of distribution was used for the solar-irradiation parameter (Q^*). Three distributions of this parameter were assigned, corresponding to three specific times: 1950, 12,000 yr B.P., and 18,000 yr B.P. (table 6). The data for 1950 represent the present reference state; the data for 12,000 yr B.P. represent the time at or shortly after maximum lake levels recorded in the Lahontan and Mono basins; and the data for 18,000 yr B.P. represent the time of maximum worldwide glacial accumulation (fig. 2). In terms of seasonal deviation of solar irradiation, the situation 18,000 yr B.P. was very similar to the situation in 1950; however, winter solar irradiation was at a minimum, and summer solar irradiation was at a maximum 12,000 yr B.P. (fig. 8).

Table 6.--*Solar irradiation for the 21st of each month at 40° north latitude for 1950, 12,000 years before present, and 18,000 years before present*

[yr B.P., years before present]

Date	Calories per centimeter squared per day		
	1950	12,000 yr B.P.	18,000 yr B.P.
January 21----	374	343	373
February 21---	513	489	521
March 21------	690	689	711
April 21------	852	887	884
May 21--------	961	1,030	994
June 21-------	996	1,080	1,019
July 21-------	954	1,024	958
August 21-----	842	879	829
September 21--	680	682	660
October 21----	507	484	488
November 21---	372	341	359
December 21---	322	289	315

A listing of the various parameter distributions, as well as the change allotted to a given parameter used in the sensitivity analysis, is shown in table 7. Note that values for dew-point temperature have been replaced with equivalent values of relative humidity to aid the reader in understanding the magnitude of the change in terms of a familiar parameter.

Mean optical air mass ($\overline{M}$), and air pressure (P), are relatively invariant with time; therefore they were held constant in the sensitivity analysis. For the purpose of the sensitivity analysis, the advected heat energy was assumed equal and opposite in size to the mean annual change in stored heat energy (eq. 43).

Table 7.--*Values of parameters used in evaporation-sensitivity analysis*

[Values refer to differences relative to reference data set (table 3); month following value indicates time at which difference was maximized for a scaled-parameter distribution; °K, degrees Kelvin; f_{hl}, fraction of high-level clouds; f_{ml}, fraction of medium-level clouds; f_{ll}, fraction of low-level clouds]

Air temperature (°K)	Water temperature (°K)	Relative humidity (percent)	Sky-cover amount (percent)	Cloud Type		
				f_{hl}	f_{ml}	f_{ll}
0	0	0	0	0.80	0.10	0.10
-5 July	-5 July	-10	+10 August	.70	.20	.10
-10 July	-10 July	-20	+20 August	.70	.10	.20
-15 July	-5	+10	+10 January	.60	.30	.10
-5	-10	+20	+20 January	.60	.20	.20
-10			+10	.50	.40	.10
			+15	.50	.30	.20
			+20	.50	.20	.30
				.40	.30	.30
				.33	.33	.33

Parameter Combinations

In the sensitivity analysis, the reference data set (table 3) was run, using three different values of Q* combined with the nine variations in $f_{hl} : f_{ml} : f_{ll}$ (tables 6 and 7). Having demonstrated the effect of Q* on evaporation rate, all subsequent computer calculations were done, using the 12,000-yr B.P. value of Q*, combined with various combinations of the values of T_a, T_o, RH, χ, and $f_{hl} : f_{ml} : f_{ll}$. A total of about 6,000 evaporation calculations were made, using the EVAP computer program. The EVAP computer program represents a major refinement to an earlier energy-flux balance model developed by Benson (1981). Improvements include:

1. Incorporation of more accurate series approximations for e_s and e_a in terms of T_a and T_{dp} (Lowe, 1977);

2. Explicit treatment of the dependence of RH on both T_a and T_{dp};

3. Inclusion of the dependence of Q_a on f_{hl}, f_{ml}, f_{ll}, α_{hl}, α_{ml}, and a_{ll};

4. Values of Q* based on a solar constant of 1.94 λ min^{-1}; and

5. Use of the EVAP computer program to calculate all components of the energy-flux balance, except Q_v and ΔQ_v.

Results of Sensitivity Analysis

In former studies (for example, Galloway, 1970), great emphasis has been placed on decrease of evaporation rate due to air-temperature reduction. However, the sensitivity analysis showed that evaporation rate does not change when both T_a and T_o are reduced by equal amounts. For example, reduction of both July T_a and July T_o by 10 °K resulted in a calculated evaporation rate of 1.18 m yr^{-1}, which is nearly identical to the rate calculated using reference-state data--that is, 1.17 m yr^{-1}. Therefore, the difference between T_a and T_o--that is, T_a-T_o--is the fundamental thermal parameter affecting evaporation. A change in air temperature alone does not necessarily indicate a change in evaporation rate.

Certain computed evaporation data sets are given in table 5. The data are ordered so the maximum computed rate of evaporation is located at the upper left of the table, and the minimum computed rate of evaporation is located at the lower right of the table. The range of computed rates is significant, ranging from 0.266 to 1.166 m yr^{-1}.

The response of the computed evaporation rate to change in each of the climate parameters is summarized in figure 9. Several conclusions can be drawn from these data:

1. Evaporation rate is most dependent on the thermal parameter, T_a-T_o. For example, monthly decreases of 5 and 10 °K in T_a-T_o result in evaporation-rate reductions of 0.35 and 0.58 m yr^{-1}.

2. Use of solar-irradiation values for 12,000 and 18,000 yr B.P. result in small increases in the computed rate of evaporation.

3. Relatively large absolute changes in relative humidity (RH) result in rather small changes in the computed rate of evaporation. For example, an extrapolated monthly increase of relative humidity by 40 percent increases the relative humidity of the dryest month (July) to 64 percent, while 4 of the more humid months acquire humidities in excess of 95 percent; however, the calculated mean annual evaporation rate decreases by only 0.06 m.

4. Change in the fractional distribution and absolute amount of sky cover can result in a significant reduction in the computed evaporation rate.

POSSIBLE CAUSES OF EVAPORATION-RATE REDUCTION IN THE LAHONTAN BASIN 14,000 TO 12,500 YEARS AGO

It has been stated previously that, given a mean-annual fluid input to the Lahontan Basin equivalent to the fluid input occurring in 1969, the creation and maintenance of the last highstand lake necessitated a reduction in evaporation rate to 0.46 m yr^{-1}. The following discussion will attempt to associate the reduction of evaporation rate to changes in certain climate parameters.

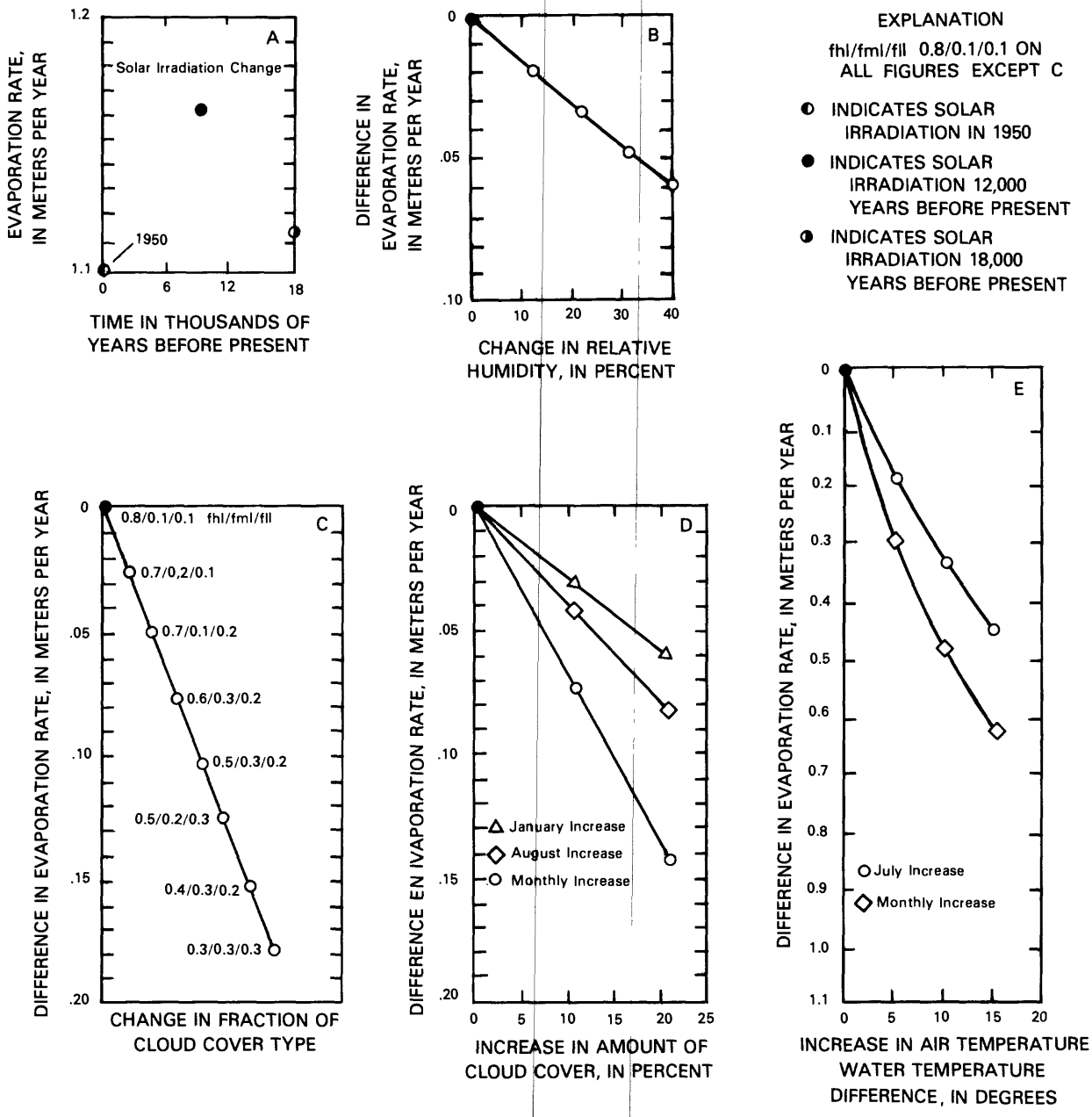

Figure 9.--Evaporation as a function of: *A*, solar irradiation (Q*); *B*, relative humidity (RH); *C*, cloud-cover type--fraction of high-level clouds (f_{hl}), fraction of medium-level clouds (f_{ml}), and fraction of low-level clouds (f_{ll}); *D*, amount of sky cover (χ); and *E*, $\Delta T_a - T_o$, increase in the difference between air temperature (T_a) and water temperature (T_o).

Air Temperature

Results of paleobotanic and geomorphic studies, previously cited, indicate a decrease of mean annual air temperature by 7 °K. Results of the sensitivity analysis (summarized in fig. 9) indicate that reducing the mean monthly air temperature by 7 °K results in a decrease of evaporation rate to 0.72 m yr^{-1}, with $f_{hl} : f_{ml} : f_{ll}$ set to 0.8 : 0.1 : 0.1, and lake-surface temperatures set to present-day values. If the 7 °K reduction in mean annual air temperature is distributed in a scaled manner, with a maximum reduction of 15 °K occurring in July, and no reduction occurring in January, and under the same conditions of water temperature and fractional sky cover as stated previously, the evaporation rate is reduced to about 0.64 m yr^{-1} (table 5). This indicates that a reduction of 7 °K in mean annual air temperature is not sufficient to lower the evaporation rate to 0.46 m yr^{-1}.

Cloud Cover

Increases in the amount and type of cloud cover, relative to values used in the historical reference set, combined with an increase in the difference between air and water temperature, can result in evaporation rates $\leq$0.46 m yr^{-1}. The data set for 15 °K in table 5 illustrates this effect. For sky-cover increases of 20 percent each month, 7 of 10 cloud distributions have computed evaporation rates of $\leq$0.46 m yr^{-1}.

Water Temperature

Before continuing, it should be pointed out that the assumption that mean-annual air temperature will decrease without a corresponding proportional decrease in mean-annual water-surface temperature probably is erroneous, because experience indicates that the colder the air, the colder the lake. This means that a reduction by 7 °K in mean-annual air temperature does not necessitate an increase in the air-water temperature difference (T_a-T_o) by 7 °K. This has significant consequences in terms of fixing the cause of evaporation reduction in the Lahontan basin from 14,000 to 12,500 yr B.P. If, for example, T_a-T_o changed by only 5 °K each month, only the most extreme conditions of cloudiness considered in the sensitivity analysis result in calculated evaporation rates of $\leq$0.46 m yr^{-1} (table 5). Other physical processes, such as ice cover, may have to be considered to account for the highstand of Lake Lahontan 14,000 to 12,500 yr B.P.

SUMMARY AND CONCLUSIONS

In this paper, the data indicate that evaporation may have had a substantial effect in the creation and maintenance of highstands of paleolakes, such as Lake Lahontan. Using precipitation and runoff data for a particularly wet year as a proxy for mean-annual fluid input 14,000 to 12,500 yr B.P., calculations indicate that evaporation had to have been reduced to about 40 percent of its present-day value to support the large surface area of Lake Lahontan.

To assess the sensitivity of evaporation rate to variation in climate, a review of evaporation methods was made. The energy-balance method was determined to be the most useful, as evaporation could be calculated as a function of commonly measured climatic parameters (air temperature, water temperature, solar irradiation, humidity, fraction of sky cover, and amount of sky cover).

Results of the sensitivity analysis indicated evaporation rate to be most dependent on the difference in air and water temperature as well as the type of clouds and degree of cloudiness. A knowledge of air temperature alone was determined to be insufficient for the estimation of paleoevaporation rates.

REFERENCES

Antevs, E., 1952, Cenozoic climates of the Great Basin: Geological Research, v. 40, p. 94-108.

Benson, L.V., 1978, Fluctuation in the level of pluvial Lake Lahontan during the last 40,000 years: Quaternary Research, v. 9, p. 300-318.

_____1981, Paleoclimatic significance of lake-level fluctuations in the Lahontan Basin: Quaternary Research, v. 16, p. 390-403.

_____1984, Hydrochemical data for the Truckee River drainage system, California and Nevada: U.S. Geological Survey Open-File Report 84-440, 35 p.

Benson, L.V., and Mifflin, M.D., 1985, Reconnaissance bathymetry of basins occupied by Pleistocene Lake Lahontan, Nevada and California: U.S. Geological Survey Water-Resources Investigations Report 85-4262, 14 p.

Berger, A.L., 1978, A simple algorithm to compute long-term variations of daily or monthly insolation: Institute d'Astrononie, et de Geophysique Georges Lemgitre Universit e Catholique de Louvain, Contribution No. 18, 29 p.

Born, S.M., 1972, Late Quaternary history, deltaic sedimentation and mudlump formation at Pyramid Lake, Nevada: Reno, Nevada, Desert Research Institute, Center for Water Resources, 97 p.

Bowen, I.S., 1926, The ratio of heat losses by conduction and by evaporation from any water surface: Physical Review, v. 27, p. 779-787.

Brakenridge, G.R., 1978, Evidence for a cold, dry full-glacial climate in the American Southwest: Quaternary Research, v. 9, p. 22-40.

Broecker, W.S., and Orr, P.C., 1958, Radiocarbon chronology of Lake Lahontan and Lake Bonneville: Geological Society of America Bulletin, v. 69, p. 1009-1032.

Brutsaert, W., 1984, Evaporation into the atmosphere, theory, history, and applications: Boston, D. Reidel Publishing Co., 299 p.

Bryson, R.A., and Hare, F.K., 1974, The climates of North America, chap. 1 *of* Bryson, R.A., and Hare, F.K., eds., Climates of North America [Volume 11 *of* Landsberg, H.E., ed., World Survey of Climatology (series)]: New York, Elsevier, p. 1-47.

Currey, D.R., and Oviatt, C.G., 1985, Durations, average rates, and probable cause of Lake Bonneville expansions, stillstand, and contractions during the last deep-lake cycle, 32,000 to 10,000 years ago, *in* Kay, P.A., and Diaz, H.F., eds., Problems of and Prospects for Predicting Great Salt Lake Levels: Salt Lake City, University of Utah, Center for Public Affairs and Administration, p. 1-9.

Dalton, J., 1802, Experimental essays on the constitution of mixed gases; on the force of steam or vapor from water and other liquids in different temperatures, both in a Torricellian vacuum and in air; on evaporation and on the expansion of gases by heat: Manchester Literary and Philosophical Society Memoirs, v. 5, p. 535-602.

Davies, J.A., Schertzer, W., and Nunez, M., 1975, Estimating global solar radiation: Boundary-layer meteorology, v. 9, p. 33-52.

Dohrenwend, J.C., 1984, Nivation landforms in the western Great Basin and their paleoclimatic significance: Quaternary Research, v. 22, p. 275-288.

Everett, D.E., and Rush, F.E., 1967, A brief appraisal of the Walker Lake area, Mineral, Lyon, and Churchill Counties, Nevada: U.S. Geological Survey Water Resources Reconnaissance Series Report 40, 41 p.

Galloway, R.W., 1970, The full-glacial climate in the southwestern United States: Association of American Geographers Annual, v. 60, p. 245-256.

Harbeck, G.E., Jr., 1962, A practical field technique for measuring reservoir evaporation utilizing mass-transfer theory: U.S. Geological Survey Professional Paper 272-E, p. 101-105.

Harding, S.T., 1965, Recent variations in the water supply of the western Great Basin: University of California--Berkeley, Archive Series Report 16, 226 p.

Houghton, H.G., 1954, On the annual heat balance of the northern hemisphere: Journal of Meteorology, v. 11, p. 1-9.

Houghton, J.G., Sakamoto, C.M., and Gifford, R.O., 1975, Nevada's weather and climate: Nevada Bureau of Mines and Geology Special Publication 2, 150 p.

Kasten, F., 1966, A new table and approximation formula for the relative optical air mass: Archiv für Meteorologie, Geophysik, and Bioklimatologie, Serie B, band 14, w. heft, p. 206-223.

King, Clarence, 1878, United States geological explorations of the fortieth parallel, v. 1, Systematic geology: Washington, D.C., U.S. Government Printing Office, 803 p.

LaMarche, V.C., Jr., 1974, Paleoclimatic inferences from long tree-ring records: Science, v. 183, p. 1043-1048.

Leopold, L.H., 1951, Pleistocene climate in New Mexico, American Journal of Science, v. 249, p. 152-168.

List, R.J., 1951, Smithsonian meteorological tables (6th ed.): Washington, D.C., Smithsonian Institute, Smithsonian miscellaneous collections, v. 114, 527 p.

Lowe, P.R., 1977, An approximation polynomial for the computation of saturation vapor pressure: Journal of Applied Meteorology, v. 16, p. 100-103.

Mifflin, M.D., and Wheat, M.M., 1979, Pluvial lakes and estimated pluvial climates of Nevada: Nevada Bureau of Mines and Geology Bulletin 94, 57 p.

Penman, H.L., 1948, Natural evaporation from open water, bare soil, and grass: Royal Society of London Proceedings, v. A193, p. 120-146.

Priestley, C.H.B., and Taylor, R.J., 1972, On the assessment of surface heat flux and evaporation using large-scale parameters: Monthly Weather Review, v. 200, p. 81-92.

Quinn, F.H., 1979, An improved aerodynamic evaporation technique for large lakes with application to the Interntational Field Year for the Great Lakes: Water Resources Research, v. 15, p. 935-940.

Reeves, C.C., Jr., 1973, The full-glacial climate of the southern High Plains, west Texas, Journal of Geology, v. 81, p. 693-704.

Reitan, C.H., 1963, Surface dew point and water vapor aloft: Journal of Applied Meteorology, v. 2, p. 766-779.
Russell, I.C., 1885, Geological history of Lake Lahontan, U.S. Geological Survey Monograph 11, 288 p.
Sellers, W.D., 1965, Physical climatology: Chicago, University of Chicago Press, 272 p.
Slatyer, R.O., and McIlroy, J.C., 1967, Practical microclimatology: Melbourne, Australia, CSIRO, 310 p.
Snyder, C.T., and Langbein, W.B., 1962, The Pleistocene lake in Spring Valley, Nevada, and its climatic implications: Journal of Geophysical Research, v. 67, p. 2385-2394.
Spaulding, W.G., Leopold, E.B., and Van Devender, T.R., 1983, Late Wisconsin Paleoecology of the American Southwest, *in* Porter, S.C., ed., Late Quaternary environments of the United States, v. 1, The Late Pleistocene: Minneapolis, University of Minnesota Press, p. 259-293.
Stelling, E., 1822, 'Ueber die Abhängigkeit der Verdunstung des Wassers von seiner Temperatur und von der Feuchtigkeit und Bewegung der Luft (vorgelegt 1881): St. Petersburg, Repertorium für Meteorologie, Kaiserliche Akademie der Wissenschaften (Meteorologicheskii Sbornik, Imperatorskoj Akademii Nauk) v. 8, p. 1-49.
Swift, L.W., 1976, Algorithm for solar radiation on mountain slopes: Water Resources Research, v. 12, p. 108-112.
Thompson, R.S., 1984, Late Pleistocene and Holocene environments in the Great Basin: Tucson, University of Arizona, unpublished Ph. D. dissertation, 256 p.
Thompson, R.S., Benson, L.V., and Hattori, E.M., 1986, A revised chronology for the last Pleistocene lake cycle in the central Lahontan Basin: Quaternary Research, v. 25, p. 1-9.
Thompson, R.S., and Mead, J.I., 1982, Late quaternary environments and biogeography in the Great Basin: Quaternary Research, v. 17, p. 39-55.
U.S. Department of Commerce, National Oceanographic and Atmospheric Administration, 1966-74, Climatological data--National summary: Asheville, N.C., Environmental Data Service, National Climatic Center, published annually.
U.S. Geological Survey, 1884-1950, Compilation of records of surface water of of the United States through September 1950. Part 10, The Great Basin: U.S. Geological Survey Water-Supply Paper 1314, 485 p.
_____1950-60, Compilation of records of surface water of the United States, October 1950 to September 1960. Part 10, The Great Basin: U.S. Geological Survey Water-Supply Paper 1734, 318 p.
U.S. Geological Survey, 1954, Water-loss investigations--Lake Hefner studies, technical report: U.S. Geological Survey Professional Paper 269, 158 p.
_____1958, Water-loss investigations--Lake Mead studies, technical report: U.S. Geological Survey Professional Paper 298, 100 p.
_____1961-83, Water Resources Data for Nevada and California (1961-84): U.S. Geological Survey Water-Data Report Series.
U.S. Weather Bureau, 1950-65, Climatological data--National summary: Asheville, N.C., Environmental Data Service, National Climatic Center, published annually.
Van Denburgh, A.S., Lamke, R.D., and Hughes, J.L., 1973, A brief water-resources appraisal of the Truckee River basin, western Nevada: U.S. Geological Survey Water Resources Reconnaissance Series, Report 57, 122 p.

☆ U. S. GOVERNMENT PRINTING OFFICE: 1986—672-331/45264 REGION NO. 8